2012

# EFFECT OF IONIC SURFACTANTS ON ELECTROSTATIC CHARGING OF SPRAY DROPLETS

Mark T. Warren
*University of Kentucky*, markthomaswarren@gmail.com

STUDENT AGREEMENT:

I represent that my thesis or dissertation and abstract are my original work. Proper attribution has been given to all outside sources. I understand that I am solely responsible for obtaining any needed copyright permissions. I have obtained and attached hereto needed written permission statements(s) from the owner(s) of each third-party copyrighted matter to be included in my work, allowing electronic distribution (if such use is not permitted by the fair use doctrine).

I hereby grant to The University of Kentucky and its agents the non-exclusive license to archive and make accessible my work in whole or in part in all forms of media, now or hereafter known. I agree that the document mentioned above may be made available immediately for worldwide access unless a preapproved embargo applies.

I retain all other ownership rights to the copyright of my work. I also retain the right to use in future works (such as articles or books) all or part of my work. I understand that I am free to register the copyright to my work.

REVIEW, APPROVAL AND ACCEPTANCE

The document mentioned above has been reviewed and accepted by the student's advisor, on behalf of the advisory committee, and by the Director of Graduate Studies (DGS), on behalf of the program; we verify that this is the final, approved version of the student's dissertation including all changes required by the advisory committee. The undersigned agree to abide by the statements above.

Mark T. Warren, Student

Dr. Asit K. Ray, Major Professor

Dr. Steven E. Rankin, Director of Graduate Studies

# EFFECT OF IONIC SURFACTANTS ON ELECTROSTATIC CHARGING OF SPRAY DROPLETS

---

THESIS

---

A thesis submitted in partial fulfillment of the
requirements for the degree of Master of Science in the College of
Chemical Engineering
at the University of Kentucky

By

Mark T. Warren

Lexington, Kentucky

Director: Dr. Asit K. Ray, Professor of Chemical Engineering

Lexington, Kentucky

2012

# ABSTRACT OF THESIS

## EFFECT OF IONIC SURFACTANTS ON ELECTROSTATIC CHARGING OF SPRAY DROPLETS

Dust capture for small coal particles (<2.5 μm) can be improved if one takes advantage of electrostatic charges that resides on the surface of coal dust particles and on the surface of water spray droplets used to capture coal dust. Traditional dust capture methods that use water sprays are ineffective in capturing small dust particles since the motion of small dust particles is governed by electrostatic forces. If additives such as ionic surfactants could be added to water that would enhance the surface charge on water spray droplets, dust capture with water sprays could be improved.

The results presented show that n-sodium octyl sulfate causes the greatest charge enhancement versus the longer chained n-sodium dodecyl sulfate and n-sodium octadecyl sulfate. This can be explained by considering the factors that lead to droplet charge enhancement. Those factors are the mass of surfactant ions at the droplet surface, and the diffusion rate of the surfactant ions from the bulk droplet to the surface of the droplet. Sodium octyl sulfate will have a faster diffusion rate to the droplet surface because of its relatively short length, and will also maximize the mass balance of surfactant ions at the drop surface.

KEYWORDS: Dust capture; Coulombic attraction; Droplet charge; Ionic surfactants

Mark T. Warren
Mark T. Warren

February 1, 2012

# EFFECT OF IONIC SURFACTANTS ON ELECTROSTATIC CHARGING OF SPRAY DROPLETS

By
Mark T. Warren

Asit K. Ray
Director of Thesis

Steven E. Rankin
Director of Graduate Studies

February 1, 2012

# ACKNOWLEDGEMENTS

This thesis is the product of individual work, but has been influenced and benefited from the input and support of several people. First and most importantly, I would like to thank my research advisor, Dr. Asit K. Ray. Dr. Ray has provided me with knowledge and direction throughout my project and has also shown patience and understanding with my work. I would also like to thank the professors that I studied under at the University of Kentucky's Department of Chemical Engineering. Finally, I would like to thank my family for their support in helping me reach my educational goals.

# Table of Contents

# List of Tables

# List of Figures

# Chapter 1
# Introduction

The study of electrostatic charge on aerosol particles can lead to a better understanding of dust suppression in many relevant processes, and a better understanding of the electrostatic charge on the particles could lead to improved methods for dust capture. Effective dust suppression is very important in keeping workers in many industries healthy. In many industries such as mining, semiconductor processing, and pharmaceutical manufacturing, the electrostatic charge on the generated aerosols can affect the success or failure of the dust abatement process. One process of particular concern is in the area of dust abatement in underground coal mines. When coal is mined, dust is generated. Traditionally, an aqueous solution is sprayed into the air to capture the dust, and then the dust-laden water droplets settle down.

Over time, a better understanding of dust inhalation hazards has led to concern regarding dust particles with diameters of 2.5 μm and less (Lippmann 1977). Airborne dust particles of this size can travel deep into the respiratory tract and permanent lung damage can occur (Fuchs 1964). Once these small dust particles enter the lungs, they remain there, and lead to health problems such as coal worker pneumoconiosis, also known as black lung disease. Most dust particles of this size cannot be captured with traditional methods such as water sprays and, therefore, this dust will remain in the air and increases the exposure risk to workers. As stated above, water sprays are not effective in removing these small particles. This is because small, freshly mined coal dust particles are inertialess and also have an electrostatic surface charge. Sprayed water droplets carry little to no electrostatic charge. The net effect is a repulsive force between the water

droplets and the coal dust since as a neutral droplet approaches a charged particle, counter ions orient themselves to have the lowest entropy possible, leaving charges of the same polarity on both surfaces (Evans 1999). In the end, the dust intended to be captured by the water droplet never collides with the water droplet, and a successful collision between the dust particle and the water spray droplet is the first step in successful dust capture.

The first step to improving a dust capture process is to be able to quantitatively measure the success of the process. To quantify the success of a dust capture system, a parameter called collection efficiency, $\eta$, has been developed. Collection efficiency is defined as the number of dust particles collected by a water droplet, divided by the total number of dust particles that the water droplet will encounter. Ray and Dhariwal (1993) have shown that the maximum collection efficiency of dust particles 1 μm in diameter by an uncharged 20 μm diameter water droplet will not exceed 0.1, whereas the collection efficiency can exceed 10,000 if the water droplet is charged. By charging water droplets, one can take advantage of the coulombic attraction between the charged droplets and the charged coal dust particles. For dust particles with diameters of 2.5 μm and smaller, it has been shown that the only force they will experience is the electrostatic force, but, as stated above, water spray droplets have little or no surface charge. Therefore, the goal of this research is to determine if water droplets can be artificially charged using additives mixed in the bulk water solution used for generating the spray. If water spray droplets can be artificially charged with a polarity opposite to the polarity of the dust particles, dust capture can be greatly improved.

The types of additives used in this research were ionic surfactants. It is a fact that surfactants have the ability to wet the hydrophobic coal (Zeller 1983), but very little has been published about the surfactant's ability to enhance the electrostatic charge on the water droplet s surface, thus increasing the chances of a successful collision between the spray droplet and the dust particle. Ionic surfactants have been shown to increase and modify the electrostatic charge on water droplets (Polat 2000, Chein 2004), but the information in the literature remains limited. We intend to gain a further understanding of the role that surfactants play in enhancing electrostatic charge of aqueous spray droplets. To study the potential of surfactants in enhancing droplet surface charge, an experimental system was designed to (1) measure the electric charge carried by generated spray droplets, and (2) to characterize the generated droplets. A thorough understanding of these factors is needed to determine if a given surfactant enhances and modifies droplet charge.

Four surfactants were used in this study. One was a cationic surfactant, the cocoamine, with the other three all being anionic surfactants with very similar structures, differing only in the length of the hydrocarbon chains in their respective molecules. Two different droplet generators were used and data are reported from both.

The four surfactants used were cocoamine (CAM), which is a polyethoxylated tallow amine, sodium n-octyl sulfate (SOS), sodium n-dodecyl sulfate (SDS), and sodium n-octadecyl sulfate (SODS). The spray generators used were an ultrasonic atomizing sprayer (UAS) and a Vibrating Orifice Aerosol Generator (VOAG).

The objective of this research is to determine if surfactants will enhance the electrostatic charge of water droplets, and to what extent, and to determine if the polarity of the

surface charge of the spray droplets could be changed, since some coal dust will have a positive surface charge, and some will have a negative surface charge. If an electrostatic charge enhancement can be attained, then it is a fact that dust capture will be improved. We approached the study looking for methods to modify and enhance surface charge on aqueous droplets. Our literature review led us to believe that the effect of ionic surfactants on the electrostatic charge on spray droplets is governed by three properties of the respective surfactant. They are,

a) Surfactant ion density per unit area on the droplet surface due to surfactant molecules at the surface.
b) Depth of charge on the droplet surface layer.
c) Flux of the surfactant molecules from the inner region of the droplet to the droplet surface.

The properties listed in (a) and (b) represent a mass balance of the surfactant ions on the surface layer of the water droplet, and (c) is the flux of the surfactant to the surface and is influenced by (a) and (b), due to Marangoni effects.

During the study, we also learned that droplet charge polarity can be manipulated under the proper experimental conditions, which is important because coal dust, or any airborne particle, can be either positively charged, or negatively charged.

This thesis is organized as follows. The first two sections contain the lists of tables and figures, followed by Chapter 1, which is the introduction. In Chapter 2, a review of the dust capture theory and electrostatic charge on dust particles is given. Chapter 2 will also review the theory of electrostatic charge on the surface of water droplets and the theory behind methods to enhance and modify the surface charge using additives. Chapter 3

discusses in detail the experimental system, and Chapter 4 discusses methods of data analysis. Chapter 5 contains the results and discussion, and Chapter 6 contains conclusions and future work.

# Chapter 2
# Theoretical Background

## 2.1 Introduction

For coal dust to be captured with a water spray, a collision between the dust particles and the water droplets must occur. Dust particles with diameters of 2.5 μm and smaller rarely collide with the water spray droplets due to the fact that dust particles of this small size have no inertia. The coal dust particles also carry an electrostatic charge on the surface and the water droplets carry little or no surface charge. Several investigators (Kraemer and Johnstone 1955; Nielsen and Hill 1976; Dhariwal, Hall, and Ray 1993) have shown that only electrostatic forces govern the motion of aerosol particles of diameters less than 2.5 μm. In this chapter, a review of the theory behind dust capture is performed, as well as a review of the theory of surface charging of droplets generated by sprays, both with and without additives.

Newly formed water droplets generated from the breakup of a liquid column will have a surface charge imbalance due to excess electrons or protons left on newly formed droplets since surface renewal rates are not as fast as the shearing rate of the liquid that is broken up into drops. Coal dust particles also have surface charges (Mukherjee et. al. 1987; Kwetkus et. al. 1993) due to the triboelectrification of the bulk coal being broken up into coal fragments and coal dust. In the last section of this chapter, a review of the theory of enhancing and modifying the natural charging of water sprays through the use of surfactants or ionic compounds is presented. Polat (2000) and Chein (2004) have shown that the addition of surfactants to water can increase the electrostatic charge on water droplets, but only at low surfactant concentrations.

## 2.2 Dust capture theory

Effective dust capture can determine the success or failure of many important industrial processes, as discussed above. Increasing concern is being shown over the lack of effective technologies to capture dust with particle diameters less than 2.5 μm. In order to determine the effectiveness of any given dust capture process, Kraemer and Johnstone (1955) proposed a quantitative measure of this dust capture effectiveness and called it the collection efficiency, η. The collection efficiency is defined as the ratio of the number of dust particles captured by a collector droplet to the number of particles that the collector droplet encounters. The mathematical equation for collection efficiency, as reported by Ray and Dhariwal (1993) is given by

$$\eta = \oint \frac{J \cdot dS}{[\pi(R_c + R_p)^2 U_r N]} \tag{2.1}$$

where $J$ is the particle flux to the surface of the collector, $R_c$ is the collector radius, $R_p$ is the particle radius, $N$ is the particle concentration in the bulk gas phase, and $U_r$ is the relative velocity between the collector and the particle. In this study $U_r$ is assumed to be the velocity of the bulk gas since the particles being investigated are small enough that they immediately attain the same velocity as the bulk gas. See Figure 2-1 for a better understanding of how collection efficiency is defined.

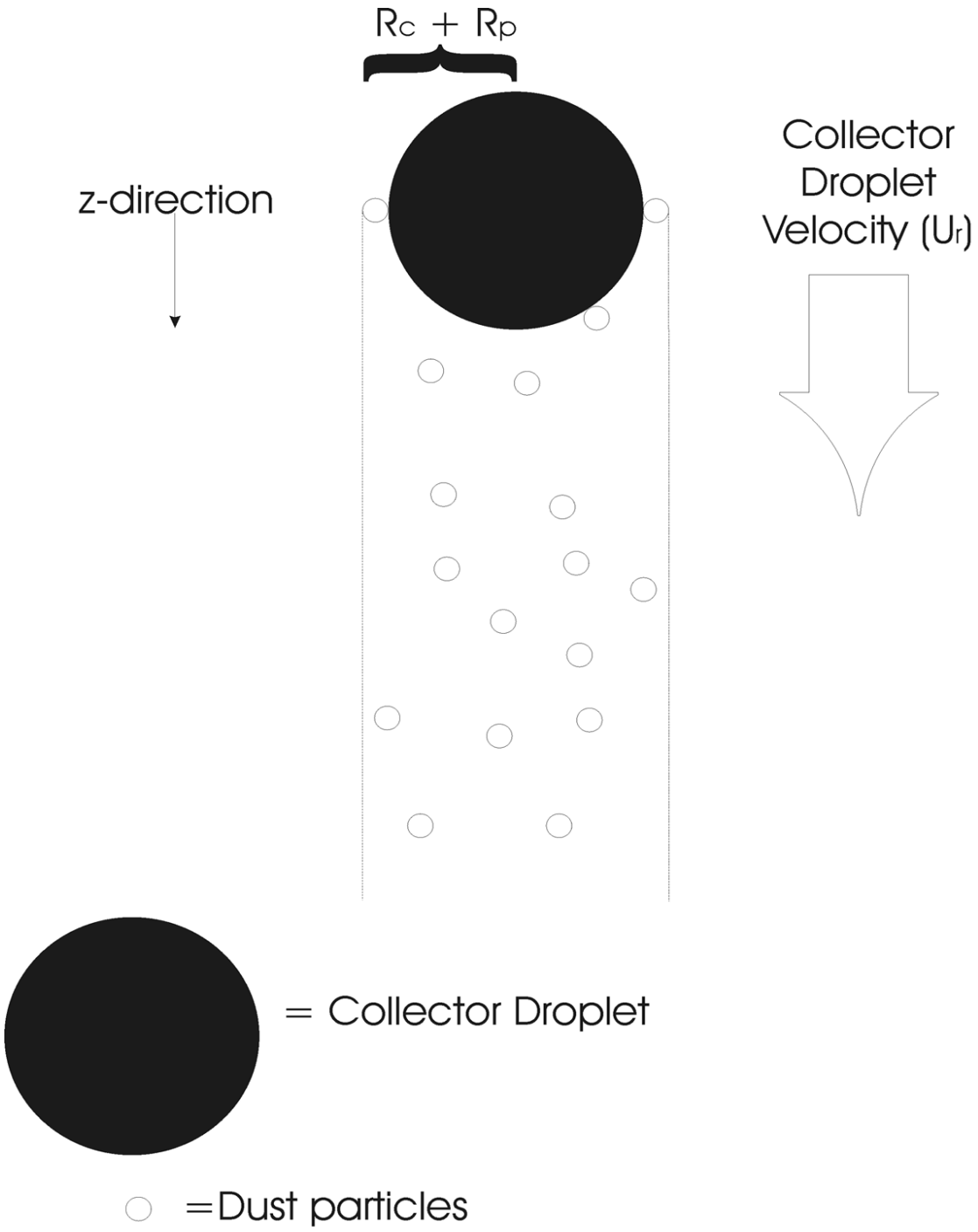


Figure 2-1: The collection efficiency is defined as the number of dust particles captured by the collector droplet divided by the number of dust particles that the collector droplet encounters. As the collector droplet settles in air, it will come in close contact with all dust particles in an imaginary cylinder that defines its flow path, but few dust particles will actually collide with the collector droplet.

To solve the surface integral of equation 2.1, the equation of motion needs to be solved for every dust particle that the water droplet will encounter. According to Fuchs (1964), dust particles in our size range of interest have Reynolds numbers approaching zero and therefore can be modeled as

$$\frac{4}{3}\pi R_p^3 \rho_p \frac{d\boldsymbol{v}}{dt} = -\left(\frac{6\pi\mu R_p}{C}\right)(\boldsymbol{v}-\boldsymbol{u}) + \sum \boldsymbol{F}_e \qquad (2.2)$$

where $R_p$ is the particle radius, $\rho_p$ is the particle density, $\boldsymbol{v}$ is the particle velocity (a vector), $\mu$ is the viscosity of the bulk fluid, $\boldsymbol{u}$ is the bulk fluid velocity (a vector), $C$ is the Cunningham correction factor, and $\boldsymbol{F_e}$'s are the electrical forces acting on the particle (vectors). The Cunningham correction factor can be neglected since all particles and droplets we are studying are very close in size. Equation 2.2 is very difficult to solve because each dust particle is influenced by several forces, but many researchers have shown that many of these forces can be neglected. In 2.2, Nielsen and Hill (1976a) and Fuchs (1964) showed that the left hand side of the equation will be equal to zero for particles of 2.5 μm and smaller since they are inertialess, i.e., their mass is negligible. The first term on the right hand side of 2.2 will reduce to zero since inertialess particles have relaxation times on the order of $10^{-5}$ seconds and therefore instantly attain the velocity of the bulk fluid, so $\boldsymbol{v}=\boldsymbol{u}$. Equation 2.2 now simplifies to

$$\sum F_e = 0 \qquad (2.3)$$

The electrical forces that can act on a particle are the coulombic forces, the electrical image forces, the external electric field forces, and the electric dipole interaction forces [Nielsen and Hill 1976b]. In this research, only coulombic forces were considered because the dust particles and the water droplets were not subjected to an external electric field, and the coulombic forces are orders of magnitude larger that both electric dipole

interaction forces and image forces. The fact that only coulombic forces are important in the capture of small particles leads to 2.1 being reduced to 2.4 (Kraemer and Johnstone 1955).

$$\eta = -4K_E \tag{2.4}$$

where

$$K_E = \frac{CQ_PQ_C}{24\pi^2 R_P^2 R_C \mu U_0 \epsilon_0} \tag{2.5}$$

The quantity $K_E$ is termed the electrostatic parameter for coulombic interaction and is a dimensionless quantity. It is the electrostatic force divided by the drag force for the dust particle and the dust collector. In 2.5, $C$ is the Cunningham correction factor. $Q_P$ and $Q_C$ are the charge per particle (the coal in our case) and per collector (the spray droplets), respectively. $R_P$ and $R_C$ are the radius of the aerosol particle and the radius of the collector, respectively. The free stream gas velocity and viscosity are denoted $U_0$ and $\mu$, respectively. The dielectric constant of the surrounding fluid is $\varepsilon_0$.

Experiments conducted on single charged particles with an electrodynamic balance (Ray and Dhariwal 1993) and on monodisperse droplet streams (Ray and Devarakonda 1998, 2000) showed that for particles with diameters less than 2.5 μm, the best collection efficiency that can be attained without electrostatic forces is 0.1, but collection efficiencies of over 10,000 can be attained when aerosol particles are influenced by electrostatic forces. With electrostatic forces increasing collection efficiencies by such a magnitude, further study in this field is needed.

In 2.5, the electrostatic surface charge on both the dust particle and the collector droplet are in the numerator. Increasing the surface charges on either the particle or the collector will increase collection efficiency, provided the charge on the particle and collector are

opposite in polarity. The reader can now see why the amount of charge per particle is of interest. Much has been published regarding factors that influence surface charge on coal dust particles ($Q_P$), but very little has been published on factors that influence and chemically enhance surface charge of aqueous solutions ($Q_C$). This study will focus on chemically enhancing electrostatic surface charge on spray droplets.

## 2.3 Electrostatic charge on dust particles

When coal is mined, dust is generated. Dust particles carry electrostatic charges on their surface due to the specific type of coal being mined and the method of mining the coal. The charge can be of positive polarity or negative polarity. This section is a brief review of experiments that tested surface charge on coal particles, but also includes results from charge testing on other aerosol particles, since triboelectrification/contact charging is the mechanism that causes excess charges to develop on the surface of any newly generated aerosol particles.

The magnitude and polarity of mined coal dust can widely vary due to the level of trace minerals in the carbon/hydrogen lattice of the coal, coal rank, ash content (levels of Al, Fe, and Si), the porosity of the dust particles, atmospheric humidity levels, the method of mining the coal, and even on particle size.

Mukherjee, Gidaspow, and Wasan (1987) tested surface charge of Illinois Number 6 coal and found that the iron pyrites in the coal and the coal itself will both be negatively charged after mining, but the iron pyrites have higher surface charge by an order of magnitude. This is attributed to the fact that iron pyrites are ionic in nature, while coal behaves slightly as a polar hydrocarbon. For particle diameters in the 170 μm to 350 μm range, Mukherjee et. al. reported charges on coal particles of $-3 \times 10^5$ charges per particle, while $-6 \times 10^6$ charges per particle are reported for the pyrites in the coal. They attribute the charging mechanism to triboelectrification/contact electrification.

Kwetkus and Sattler (1993) also studied surface charge levels of coal dust using seven different types of coal from the U.S.A, France, and Germany. They concluded that the surface charge is caused by triboelectrification effects. Coal particles for their

experiments were 60 μm to 90 μm in diameter, and they reported values up to 6 x $10^9$ charges per particle. The dust particles were both positively and negatively charged, mainly due to ash content.

Our testing on 25 μm coal particles at the University of Kentucky Aerosols Lab yielded results showing much lower charges per particle than previous studies. For our tests, triboelectrification effects were eliminated. Coal samples were crushed and sieved, then placed in sealed containers for testing later. The coal dust was generated by a Fluidized Bed Aerosol Generator (FBAG) with dust characterization performed by an Aerodynamic Particle Sizer and electric current generated by the coal tested with an Aerosol Electrometer. Charge levels in these experiments yielded values of 100-200 charges per particle. Polarity was positive. The reason for such low values compared to values reported by other investigators is due our samples not being subjected to triboelectrification effects.

As stated above, excess surface charges on aerosol particles can result from contact charging, which is also known as triboelectrification. Periasamy and Clayton (1991) studied the amount of excess surface charges on generated aerosol particles with the purpose of improving processes in the semiconductor manufacturing industry. Surface charge on DOP particles was tested with an electrometer, using a Vibrating Orifice Aerosol Generator (VOAG) to produce the aerosol particles. The vibration of the VOAG served as the mechanism for contact charging. Ethanol was used to solvate the DOP for initial particle generation. In cases like this, the solvent, EtOH will evaporate after the droplet is generated, leaving a particle of DOP. The DOP particle will retain any excess surface charges caused by the droplet generation. Periasamy and Clayton observed

surface charges up to 16,506 excess charges per DOP particle. Charge per particle increased as they increased the frequency of vibration of the piezoelectric crystal, which shows that the rate of liquid break up into droplets is a key factor in determining level of excess charges on particle surfaces.

Marra and Coury (2000) reported results from contact charging tests of airborne particles of methylene blue, with particle diameters in the range of 7 µm to 11.5 µm. Solid particles were generated with a Vibrating Orifice Aerosol Generator. After particle generation, the particles were accelerated through an electrostatic charge classifier where contact charging occurred. For 7 µm particles, 813 negative charges per particle are reported, and charge becomes more negative as particles get larger, but only to a point. For 8.3 µm particles, 1063 negative charges per particle are reported, but then the trend reverses and charge per particle becomes less negative. Particles with diameters of 11 µm showed no charge, and 312 positive charges per particle are reported for particle diameters of 11.5 µm. Marra and Coury theorized that excess charges on particles was a result of friction or impaction between the particles, which is a form of triboelectrification charging.

Marra and Coury (2009) continued their work testing electrostatic charge arising from contact charging/triboelectrification. In their work from 2009, they tested charges imparted on phosphate particles caused by high speed impaction with a copper disk. The rocks were 1.5 µm to 8 µm in diameter, and their results showed that imparted charge due to contact charging is significant. For 8 µm particles of phosphate, 986 charges per particle were observed after impaction. Charge testing on 8 µm particles not impacted with the copper disk only had 504 charges per particle.

## 2.4 Theory of natural charging of water sprays

When a spray is generated from a bulk liquid, the spray droplets acquire an electric charge, with the bulk solution acquiring an equal charge, but of opposite polarity to maintain electroneutrality. The terminology “natural charging” or “electrolytic charging” is used when any charge detected in the generated spray or bulk solution is due solely to the breakup of the liquid, and not due to an induced charge such as passing the generated spray through an external electric field. Natural charging occurs because the drops acquire an excess of electrons or protons due to the breakup of the bulk liquid solution. Whether a generated droplet acquires a negative or positive overall charge is determined by the method of drop generation.

One of the earliest observations of natural charging of water droplets was by Elster and Geitel (1890). Elster and Geitel noted that in the area around waterfalls, a significant amount of electrical charge could be found. Lenard (1892) followed up on the work of Elster and Geitel and also put forth the first theory attempting to explain the electrification of water droplets. Lenard described how drops acquire charge because a double layer of ions exists at the liquid-gas interface, and he termed it the electrical double layer (EDL). This layer is formed because in the bulk water phase, water molecules at the air-water interface will align with the oxygen molecules pointing out towards the air due to the lone electron pairs residing in the oxygen atoms, and the hydrogen atoms will point inward toward the bulk solution. According to Lenard, as the liquid water is broken into droplets, an excess of electrons reside in the water droplets and the bulk solution will be deficient in electrons. Lenard’s theory was borrowed from

an idea first proposed by Hemholtz when Hemholtz was doing experiments with electrical capacitors (Koenigsberger 1906).

Blanchard (1958) published results from experiments he performed in which he sought to quantify the amount of charge on drops generated from the bubbles that occur in sea water. He used a Millikan type of charge measurement system and found that drops less than 20 μm in diameter were positively charged and drops with diameters between 20 μm to 40 μm were both positively and negatively charged, with drops having about 1000 charges per drop. In 1963, he published result from a more rigorous study in which drops in the size range of 20 μm to 49 μm in diameter had virtually no negatively charged droplets. It should be noted that a relationship between bubble life (time for the bubble to break and eject drops) and the polarity of the drop was also found, with increasing bubble life determining the polarity of the charge.

Iribarne and Mason (1967) did further experiments with bursting bubbles generating water and aqueous solution droplets. Iribarne and Mason produced droplets by forcing nitrogen through a capillary that was partially submersed in a grounded vessel of water. This produced bubbles that would burst and generate water droplets. With a second stream of nitrogen, the droplets were gently directed into a metal funnel that acted as a Faraday Cup, allowing the electrostatic charge on the drops to be determined. They studied pure water droplets in the diameter range of 150 μm to 400 μm, with charges per droplet ranging from $-4.2 \times 10^7$ for the 150 μm drops, up to a value of $-9.4 \times 10^7$ for 400 μm drops. Drops produced from pure water carried a negative charge in their study. Iribane and Mason also studied the relaxation time of the electrical double layer (EDL). As discussed before, early drop charge theory stated that at the air/water interface, an

excess of electrons would be present. As new droplets form, Iribarne and Mason investigated if the EDL would have time to re-establish itself by re-aligning with the oxygen atoms of the water again residing at the air/water interface. The work of Iribarne and Mason showed that the relaxation time of the EDL was about $10^{-4}$ seconds. This was faster than the rate at which they were forming drops and they concluded that this relatively fast relaxation time explained why their pure water droplets carried a negative charge. The relaxation time will be an important phenomenon to consider when determining the polarity of droplet charge.

Jonas and Mason (1968) continued the experimental work that Iribarne and Mason began on relaxation time of the EDL by extending the experiments to include charge on droplets produced by the breakup of liquid threads produced from a vibrating stainless steel capillary. In this experiment, the charge that developed on the liquid reservoir as the thread would break up was measured. They found that at lower needle vibration frequencies, generated drops had a positive charge and the reservoir developed a negative charge, and at higher vibration frequencies the drop charge was negative. This study further shed light on the concept of relaxation time.

Byrne (1977) produced droplets with an air-blasting atomizing sprayer. His sprayer was made by orienting two needles perpendicular to each other. In one needle, the liquid would flow, and in the second needle, a jet of air was used to break up the droplets. He found that drops larger than 80 μm in diameter would have a positive charge and drops smaller than this had an equal amount of positively and negatively charged drops. Byrne further proved that the method of liquid breakup is important in determining the polarity of the droplets. Byrne reported charge per droplet results in the amount of current

generated, and, since no flow rate or number density is reported in his results, the number of excess charges per droplet cannot be deciphered.

Reischl, Devor, and John (1976) produced water droplets for charge measurement with a Vibrating Orifice Aerosol Generator (VOAG). The VOAG will be discussed further in the experimental section of this thesis, but the key point to remember with the VOAG is that it produces a monodisperse stream of droplets. This is an important point to remember since the absolute value of droplet charge will, in general, increase with increasing drop size. Investigators before Reischl and Devor did studies on polydisperse droplets streams, but these investigators studied monodisperse droplet streams. Reischl and Devor reported that 35 μm diameter drops of deionized water would have 1350 positive charges per drop. Note that the polarity of the droplet was positive. These results show that the drop production with a VOAG is faster that the relaxation time of the EDL.

Polat and Chander (2000 and 2002) produced droplets from distilled water and reported a value of 5400 charges per droplet, with 67% of the droplets having positive charge, 12% having a negative charge, and 21% of the droplets showing a neutral charge. The diameters of the droplets tested ranged from 50 μm up to 125 μm. Their droplets were generated with a spray nozzle having two inlets, one for air and one for water. The majority of their generated droplets were positive in polarity, indicating the drops were formed faster than the EDL could re-establish itself.

Zilch et. al. (2008) performed experiments on the natural charging of water droplets using both a VOAG and a sonic sprayer. It should be noted that the VOAG was constructed by the experimenters and this particular VOAG did not produce a monodisperse droplet stream. They also constructed their own sonic sprayer, which consisted of two concentric

capillary tubes, with the inner capillary being 100 µm in inside diameter, and the outer capillary having an inside diameter of 250 µm. Water was fed to the inner capillary and air flowed through the outer capillary. With their VOAG, the average size of the droplets was 114 µm in diameter, with charge levels around 2000 positive charges per drop. Drops from their sonic sprayer had an average diameter of 52 µm, with about 5000 positive charges per drop. The reader is asked to take note of the fact that drops generated by Zilch and Maze had a positive polarity, and charge levels from the sonic sprayer were over twice that of the VOAG. This finding again shows that polarity and charge level of water droplets is determined by the method of drop generation, and to a large extent, the relaxation time of the electrical double layer.

## 2.5 Modification and enhancement of droplet charge

With the addition of various chemical species to water, the electrical surface charge on generated spray droplets can be reduced, modified, or enhanced. As stated in the Introduction of this thesis, there are three factors that govern the magnitude and polarity of surface charge. First, number of ions per unit surface area on the droplet surface is important. Second, the depth of the charges on the droplet surface is important. Third, the flux of ions/surfactant molecules to the droplet surface is important. The review presented in this section is meant to accomplish two things. First, results are presented that will be compared with our results in Chapter 5, and second, this section shows that previous investigators have theorized, like we have, that the magnitude and polarity of surface charge on droplets is governed by the three factors mentioned above.

Several investigators have shown that the addition of ionic compounds to water will lead to a reduction in the surface charge on generated droplets. This is the opposite of what we are trying to do with our study on ionic surfactants, but the theory behind it is included because it can lead to a better understanding of how ionic surfactants can be used to enhance surface charge. In theory, the addition of surfactants to water will increase the charge separation between spray droplets and the bulk liquid from where the droplets were generated. This theory is based on the phenomenon that is seen in oil/water systems in which the surfactants can influence electrical properties at the oil/water interface. Proof of the charge separation concept with generated water droplets is limited, but it is known that surfactants will be concentrated at the air/water interface (Varadaraj 1992), which could lead to higher charge in aqueous surfactant spray droplets since it is the liquid surface that breaks up to form droplets. The following section will discuss

experiments performed by various investigators on electrostatic surface charge on water droplets containing ionic compounds and ionic surfactants.

The work performed by Iribarne and Mason (1967) with pure water droplets was discussed in the previous section, but these investigators also tested surface charge on droplets generated from ionic solutions made with sodium chloride, ammonium sulfate, and sodium nitrate. They tested NaCl solutions with concentrations ranging from $10^{-6}$ M through $10^{-2}$ M. The results showed that negative charge on droplets of NaCl solutions decreased as the concentration increased, up to concentrations of ~$10^{-4}$ M. Upon further increases in concentration, droplet charge turns slightly positive. A similar trend was noted with solutions of $(NH_4)_2SO_4$ and $NaNO_3$. These investigators derived a formula for predicting the amount of charge on droplets of radius $R_D$ in e.s.u.'s, given below as 2.6.

$$Q_D = -7 \times 10^3 4\pi R_D c^{\frac{1}{2}} exp\left[-\frac{1}{2} - \frac{10^6 c^{\frac{1}{2}} R_D}{9}\right] \tag{2.6}$$

In 2.6, $Q_D$ is the charge per droplet, $R_D$ is the radius of the droplet, and $c$ is the concentration of the salt.

Iribarne and Mason tested charge on droplets and derived an equation, Equation 2.6, to fit their data, but their major contribution to the study of excess surface charges on droplet surfaces is seen in the mass balance they derived for excess charges on the droplet surface,

$$Q_D = -\left(\frac{\sigma_C}{\delta}\right)\frac{4}{3}\pi {R_D}^3 \tag{2.7}$$

where $Q_D$ and $R_D$ are defined above, $\sigma_C$ is the number of ions per unit of surface area, and $\delta$ is the depth of the ion layer and is directly related to the length of the molecule.

The work of Iribarne and Mason provide an excellent starting point for the study of

excess charges on a droplet surface since they were the first to propose a mass balance of to predict droplet charge.

Vaaraslahti and Laitinen (2002) investigated the effect of ionic NaCl and NaOH concentration on spray droplet charging in a wet scrubber for improved removal of particulate matter in power plant flue gas. They used a spray nozzle with a pressurized tank of liquid to generate droplets, and measured droplet charge by connecting an ammeter to the spray nozzle. Their results were similar to what other before them found in that droplet charge decreases as the salt concentration increases. Vaaraslahti and Laitinen theorized that the ions in solution from the addition of the salts increased conductivity in the liquid, and suppressed any excess charges that might develop on the droplet surface.

Matteson (1971) performed charge measurement experiments on sprays generated with aqueous electrolyte and aqueous surfactant solutions. His system produced droplets by breaking up the liquid stream with an air jet. His experimental system consisted of two hypodermic needles arranged perpendicular to each other. Liquid at 10 ml/min was forced through one needle, and pressurized air at velocities of 71 m/s to 125 m/s was forced through the other needle. The air would break up the liquid into droplets. An electrical lead was connected to the needle carrying the liquid, with the other end of the lead being connected to an ammeter to allow current to be measured. He observed the needle carrying the liquid developed a positive charge, and, like others before him, found that the generated drops had a negative charge. Matteson also sought to shed light on the relaxation rate of the electrical double layer (EDL), although he termed it surface renewal rate. In Matteson's work, increasing the velocity of the air jet led to a reduction of

negative charge on the droplets, which implies that the EDL is not being re-established as quickly as the droplets are formed at higher air velocities. As his results are discussed, it should be noted that Matteson reported concentration in normality, which we convert to molarity for ease of comparison when looking at the data of others.

While Matteson did not report values for charge per water droplet, a value -82,000 charges per droplet can be extrapolated from his data. Matteson tested solutions of sodium dodecyl sulfate (SDS) and stearamidopropyl dimethyl-β-hydroxyethyl ammonium dihydrogen phosphate (tradename Catanac SP). Results reported by Matteson for charge enhancement on (SDS) solutions versus concentration showed the greatest charge enhancement when using $5 \times 10^{-4}$ M SDS solutions. The value he reports for this concentration of the SDS solution is -745,000 charges per droplet.

Matteson proposed a theory about the mechanism seen when excess droplet charge is generated by the break-up of a liquid surface, with the bulk of his work focusing on the flux of ions from the inner droplet to the surface of the droplet. As mentioned in the Introduction, flux of ions, or ion diffusion, to the surface of a droplet is one of three factors affecting the magnitude and sign of excess charges on the droplet surface.

Polat and Chander (2000, 2002) investigated enhancement of electrostatic charge on aqueous surfactant spray droplets in an effort to improve coal dust abatement. These investigators tested six different ionic surfactants. The two anionic surfactants tested were sodium dodecyl sulfate (SDS) and sodium dioctyl sulfosuccinate (SDOS). The four cationic surfactants tested by Polat and Chander were dodecyl amine, and three coco amines, differing in hydrocarbon chain lengths of C5, C10, and C15. They found an increase in droplet charge at dilute surfactant concentrations, with the greatest

enhancement at 5 x $10^{-5}$ M for the SDS solution. Polat attributed the increase in droplet charge to Marangoni effects. A brief discussion of Marangoni effects follows after Polat's results are presented.

With the SDS solutions tested by Polat, droplet charge increased at SDS concentrations of 1 x $10^{-6}$ M through 5 x $10^{-5}$ M, but decreasing rapidly as SDS concentrations increased above 5 x $10^{-5}$ M. Polat attributed this to the fact that as concentrations increase above 5 x $10^{-5}$ M, the concentration of surfactant gets closer to it critical micelle concentration, and the surfactants start to self-assemble. Recall that self-assembly occurs when the surfactant dissociates in solution less and less, instead wanting to stay in close contact with other surfactant molecules. This causes less surfactant molecules to be available for diffusion to the droplet surface.

For the anionic surfactants tested, SDS showed more charge enhancement versus the SDOS. Polat theorized that SDS is a straight-chain molecule whereas SDOS has branching and, therefore, the SDS will be more densely packed at the surface of the droplet, leading to a higher concentration of the anionic group at the surface of the droplet. No range for droplet diameter was reported for the surfactant solution sprays generated. It should be noted that in the study by Polat on surfactant solution droplets, they used a high-speed camera with a telescopic lens for droplet characterization. This method can lead to coincidence error since the resolution of droplets in the background can be distorted due to droplets closer to the camera lens.

Polat's method for droplet characterization could be questioned because he makes no mention of the fact that droplet count will increase dramatically and droplet size will decrease as surfactant concentration is increased above 1 x $10^{-4}$ M due to the decrease in

surface tension of the bulk aqueous surfactant solution. Kim and Kim (1997) investigated droplet changes due to the addition of surfactants and noted a reduction in drop diameter and an increase in droplet number density as surfactant concentration increased above 1 x $10^{-4}$ M. This increase in number density and decrease in drop diameter will not be seen when droplets are generated from dilute surfactant solutions because the surface tension of bulk surfactant solutions with concentrations < 5 x $10^{-5}$ M have surface tension values of 68 mN/m to 72 mN/m (Mysels 1986, Dahanayake, Cohen, and Rosen 1986), which is very close or equal to the value for pure water. These results are presented because for effective enhancement of droplet charge, concentrations of surfactant solutions used for droplet generation should be kept below 5 x $10^{-5}$ M. Our experimental results, as well as Polat's results, prove this.

Marangoni effects help explain why surfactants concentrate on droplet surfaces as the drops move in air. Shearing stresses can be produced when the surface of a liquid moves relative to the liquid layer underneath the surface of the liquid. These stresses occur because of local surface tension gradients due to the surfactant at the air/water interface and are due to the Marangoni effects (Marangoni 1871). As spray droplets are formed, surfactant molecules in the droplet will diffuse to the droplet surface and orient with the surfactant's hydrophobic end pointed towards the air and the hydrophilic end pointed inward towards the water. As the droplet falls in air, the drag force on the droplet surface will cause the surfactant to move to and concentrate at the upper hemisphere of the droplet (Bird, Stewart, and Lightfoot 2007). This movement leads to surface area on the droplet with no surfactant molecule, which allows surfactant molecules in the bulk liquid of the droplet to have space to diffuse to the droplet surface, further increasing surfactant

concentration at the droplet surface, and hence, increase surface charge. Zuiderweg and Harmens (1958) theorized that Marangoni effects play no role in systems of spray droplets in gases, but their experiments were with toluene/n-heptane and benzene/n-heptane systems. These hydrocarbons have very similar surface tensions, with the n-heptane value being 20.1 mN/m and benzene and toluene being 28.9 mN/m and 28.4 mN/m, respectively. With these hydrocarbon systems, there is no surface tension gradient. In the case of an ionic surfactant in water, there is a great difference in surface tension values. For instance, water has a surface tension of 72 mN/m, whereas pure sodium dodecyl sulfate (SDS) has a reported surface tension of 45 mN/m to 50 mN/m (Mysels 1986). The surface tension of water compared to SDS leads to a large surface tension gradient, therefore Marangoni effects play a key role in the surface behavior of falling droplets generated from aqueous surfactant solutions.

Chein, Aggarwal, and Wu (2004) investigated spray droplet charging using four different aqueous ionic surfactants solutions at concentrations of $10^{-7}$ M to $10^{-4}$ M. The anionic surfactants they used were sodium dioctyl sulfosuccinate (SDOS) and sodium dodecyl sulfate (SDS), and the cationic surfactants tested were cetylpyridinium chloride (CPC) and cetyltrimethylammonium bromide (CTAB). The spray was generated in a manner similar to the Polat method in which the spray nozzle has a liquid inlet and an air inlet with pressurized air providing the atomization. A charge enhancement for both SDS and SDOS was noted by Chein, but the enhancement reported is in the form of a higher positive surface charge, similar to what Polat reports. The SDS enhanced the surface charge more than the SDOS, and this was attributed to the straight chain structure of SDS being able to more densely pack the droplet surface versus the branched structure of the

SDOS, leading to a higher number of ions per unit of surface area, which is one of the factors that influence excess droplet surface charges. The values reported by Chein et. al. are much lower for all results reported versus other investigators. Charge per droplet for water was 4 charges per 15 μm diameter droplet. Droplet charge for the SDS solutions was greatest at 1 X $10^{-4}$ M SDS, with the value of 18 charges per droplets for the drops of 15 μm diameter.

Not all investigators subscribe to the EDL theory to explain surface charge on aqueous droplets. Myland and Oldham (2002) stated that not all charges reside on the droplet surface, but instead also occupy a diffuse layer immediately below the droplets surface. Myland and Oldham solved the Poisson-Boltzmann equation in spherical coordinates for aqueous electrolyte solutions in the form below

$$\frac{d}{dR_D}\left(R_D^2\frac{d\varphi}{dR_D}\right) = -\frac{R_D^2 e}{\varepsilon_A}[z_+ n_+ exp\{-z_+ f_B\} + z_- n_- exp\{-z_- f_B\}] \qquad (2.8)$$

where $R_D$ is the droplet radius, $\varphi$ is the local electrical potential in the droplet, $e$ is the elementary unit of charge, $\varepsilon_A$ is the dielectric constant of the aqueous solution, $z_+$ and $z_-$ are the charge numbers of the two ions from the dissociated electrolyte, $n_+$ is the cation number density in the droplet, $n_-$ is the number density of the anions in the droplet, and $f_B$ is the Boltzmann voltage factor, which is $e/k_BT$= 38.9/Volts at 298 K. Their solution showed that only about 10% of the excess charges are on the surface, with the remainder of the charge residing in the diffuse layer immediately below the surface. It should be noted that their results were for droplets generated from electrolyte solutions and not from water or aqueous surfactant solutions. As discussed above, electrolytes in water actually lower the amount of excess surface charges. Myland and Oldham's theory on the

diffuse layer could explain why electrolytes reduce surface charge. According to them, all the charge is not on the surface, which is not the case with ionic surfactants since the hydrophobic end of a surfactant molecule will orient with the hydrophobic tail of the surfactant pointing outward in the direction of the air at the air/water interface once the surfactant molecule has diffused to the droplet surface through the bulk liquid of the droplet.

# Chapter 3
# Experimental Setup and Procedure

## 3.1 Introduction

The experimental setup and procedure used in this study are intended to measure the electrostatic charge on water and aqueous surfactant spray droplets. When a spray is generated, the droplets formed have an excess of electrons or protons left on newly formed droplets. The purpose of our experiment is to measure the excess charges on the generated spray droplets.

For the study, two droplet generators are used. The first generator is an Ultrasonic Atomizing Sprayer (UAS). The second droplet generator is a Vibrating Orifice Aerosol Generator (VOAG). After the drops are generated, they are directed to a settling chamber. In the settling chamber, there is a reduction in drop size due to evaporation as the droplets settle in air, but the drops retain their surface charge. A conductive coating was applied to the settling chamber when it was constructed to reduce build up of static charge on the chamber walls. Drops are dispersed in the chamber by flowing air through the chamber using a vacuum pump. The flow rate in the settling chamber due to the vacuum pump is controlled and monitored with a rotometer. A fraction of the flow passes through an Aerosol Electrometer (AE) that is used to determine the current level on a known number of individual drops, and another fraction of flow passes through an Aerodynamic Particle Sizer (APS) that is used to determine droplet diameter and to determine the number of drops in a given volume of bulk gas. Figure 3-1 shows an overall schematic of the experimental system. Deionized water with a resistivity of 17.4 MΩ/cm was used for all

water and aqueous surfactant experiments. All surfactants used for experiments were purchased from Fisher Scientific and are more than 99% pure.

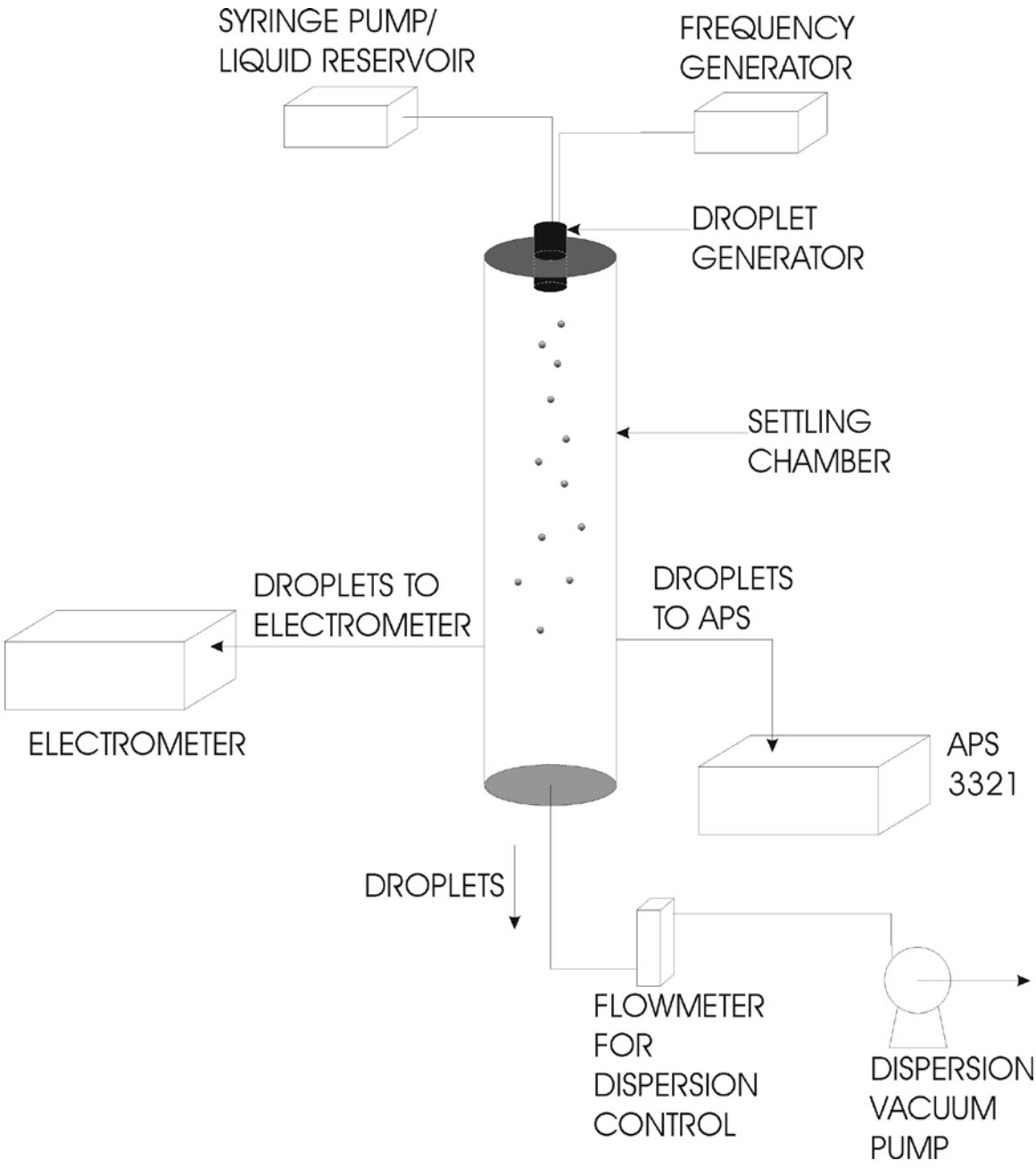


Figure 3-1: Schematic overview of the charge measurement system.

## 3.2 Droplet Generation

### 3.2.1 Ultrasonic Atomizing Sprayer (UAS)

An Ultrasonic Atomizing Sprayer (UAS) from Sonaer Ultrasonics was used for most of the experiments in the study. The UAS generates a polydisperse water spray using an atomizing nozzle and an ultrasonic frequency generator. A histogram is presented in the data analysis chapter showing the polydisperse droplet size distribution that one gets when using the UAS. The type of atomizing spray nozzle is a model 40K50ST, and the frequency generator type is the Digital Ultrasonic Generator operating with software version 3.01. The frequency describes the rate at which the nozzle vibrates axially, thereby breaking up the liquid stream. Unlike the variable frequency generator used with the VOAG, the UAS uses a fixed frequency generator. Only one frequency signal is available from Sonaer and that frequency is calibrated at the Sonaer factory based on which nozzle is used. For this study, the frequency used was 43 kHz. The frequency generator does provide a way to vary power to the sprayer. By varying power, the length of the axial vibration of the sprayer tip is can be varied (Jokanovic and Uskokovic 1999). A lower power setting causes a shorter tip vibration length, and a higher power setting causes a longer tip vibration length. Regardless of the power setting, the frequency of tip vibration remains at 43 kHz. A syringe pump from KD Scientific Model 220 is used to feed liquid to the sprayer. With this pump, liquid flow rates can be controlled to within 2%. The UAS atomizing nozzle was electrically grounded at all times so any charge build up in the bulk solution due to droplet generation would be dissipated.

The method for generating spray droplets with the UAS is as follows. Syringes are filled with 60 ml of the liquid solution to be tested, and any air bubbles caused by the filling

process are removed. This is important because of the way the molecules of the water and surfactant solutions will orient themselves at the air/water interface. The syringes are placed in the pump and the flow rate used in the experiments, 2 ml/min, is set by entering the flow rate value into the syringe pump controller. The frequency generator is turned on, causing the atomizing nozzle tip to vibrate and then the power level of vibration is set. The two power levels used in the UAS experiments were 6.8 Watts and 3.8 Watts. Power level is set by adjusting up and down arrows on the frequency generator display. The syringe pump is started and feeds liquid to the vibrating atomizing nozzle, and liquid break up occurs. Figure 3-2 shows the nozzle tip vibration pattern that occurs in the axial direction of the liquid feed. Figure 3-3 shows a picture of the generated spray.

As stated above, the UAS creates polydisperse drops. Although the spray is polydisperse, Lang's formula, shown as 3.1, will give an approximation of the mean diameter of the drops. The actual diameter varies slightly based on the power level of the ultrasonic generator.

$$D_D = 0.73\left[\frac{\sigma}{\rho_d f^2}\right]^{\frac{1}{3}} \tag{3.1}$$

In 3.1, $D_D$ is particle diameter, $\sigma$ is surface tension of the liquid being sprayed, $\rho_d$ is density of the liquid being sprayed, and $f$ if the frequency of oscillation of the nozzle for droplet breakup. When generating drops with the UAS, the frequency will vary +/- 50 Hz, and this is one of the reasons for the polydisperse droplets generated with the UAS. Once drops are being generated, the settling chamber is oriented under the sprayer, as shown in Figure 3-1. Figure 3-1 also shows how the vacuum line for the droplet dispersion system, APS, and AE are attached once the chamber is in place. The experiment was designed so it only takes about 1 minute to put the settling chamber in

place and attach the vacuum line, APS, and AE. At this point the vacuum pump is turned on and the droplets are dispersed through the column. With the measurement equipment in place and the vacuum pump on, data can now be generated. Both the APS and the AE have a vacuum pump (not shown on Figure 3-1) that pulls the droplet samples into the instruments for sample analysis. The data from the APS and the AE are used to determine the amount of excess charges per droplet and the polarity of the drops, and is discussed in the results and discussion section. How the data is analyzed to arrive at a value for excess charge per drop is discussed in the data analysis chapter.

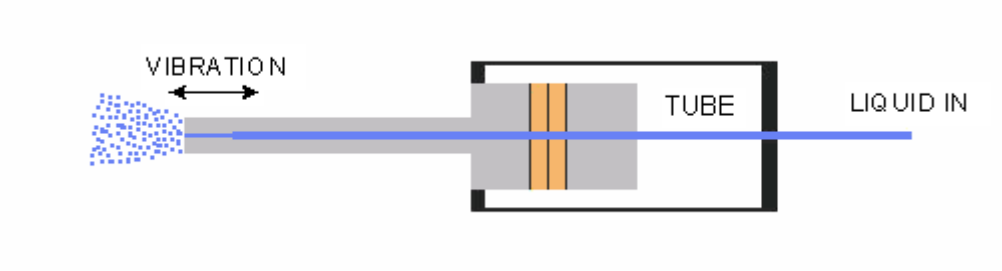


Figure 3-2: The atomizing spray nozzle vibrates axially as the liquid flows through the nozzle and the vibrating action breaks up the liquid column into polydisperse droplets. Drawing courtesy of Sonaer Ultrasonics.

Figure 3-3: This picture shows how the spray droplets are broken up from the bulk liquid solution. Picture courtesy of Sonaer Ultrasonics

### 3.2.2 Vibrating Orifice Aerosol Generator (VOAG)

The second type of droplet generator used for the charge measurement experiments is a Vibrating Orifice Aerosol Generator (VOAG). The VOAG produces a monodisperse droplet stream (Berglund and Liu 1973). The VOAG used in our experiments was modified for improved control of droplet generation. The head of our VOAG was manufactured by Thermo-Systems Instruments (TSI), with the rest of the system being made by the University of Kentucky Aerosols Lab.

The modified VOAG in our lab also produces highly monodisperse droplets (Devarakonda 1998). A histogram is presented in the data analysis chapter showing the monodisperse droplet size distribution one gets when using our VOAG.

The components of the VOAG are a pressurized ballast tank, a liquid reservoir, capillary tubes to supply liquid, electrical connections for the frequency signal, and a piezoelectric (PZT) crystal which houses the liquid chamber and the stainless steel pinhole orifice disk. A frequency synthesizer and a square wave generator provide the frequency signal that is the motivating force for droplet breakup. Figure 3-4 shows a schematic of the VOAG head. The frequency synthesizer and wave generator are not shown in Figure 3-4, but are upstream of the “generated square wave” input and generate the square wave that vibrates the PZT. The pressurized ballast tank and the liquid reservoir and also not show in this figure but are upstream of the “liquid feed” inlet on the figure.

The VOAG produces droplets by liquid flowing from the liquid reservoir to the VOAG head. Flow rates for VOAG experiments ranged from 0.21 ml/min through 0.29 ml/min. The ballast tank provides the pressure needed to force the liquid through the 20 μm pinhole orifice disk which is attached to the PZT crystal. The ballast tank pressure was 16

psi for all VOAG experiments reported in this study. A frequency signal is applied to the PZT crystal, causing it to vibrate at frequencies of 200 Hz to 80 MHz. The vibration causes the liquid stream to breakup into monodisperse droplets and the droplet diameter can be calculated from 3.2,

$$\boldsymbol{D_D = \left[\frac{6Q}{\pi f}\right]^{\frac{1}{3}}} \tag{3.2}$$

where $D_D$ is the droplet diameter, $Q$ is the liquid flow rate, and $f$ is the vibrating frequency of the orifice disk.

The VOAG system used was modified by our lab to allow a high level of control over droplet generation. Equation 3.2 shows that two variables need to be accurately controlled for stable drop generation. These are flow rate, $Q$, and frequency, $f$. This led to the first modification of the VOAG system. We use a pressurized ballast tank to control liquid flow rate to within 0.001%. The VOAG system from TSI uses a syringe pump for liquid flow rate control. A syringe pump is not capable of this precise control. Consistent monodisperse droplet generation is also dependent on stable frequency generation, $f$, also seen in equation 3.2. For this reason, a Hewlett Packard 3335A frequency synthesizer is used with our VOAG, whereas the TSI unit is sold with a function generator. This function generator can fluctuate by a few hertz, but the HP frequency synthesizer fluctuates less than 0.1 Hz. An additional improvement by our lab is the implementation of a square wave generator (Devarakonda 1998). The frequency synthesizer emits a sine wave and, consequently, the PZT crystal only receives the peak amplitude of the signal for a short time. By using a square wave generator, the PZT crystal is exposed to the peak amplitude for a longer time.

Figure 3-5 shows the VOAG head with the dispersion cap attached. The dispersion cap, coupled with the dispersion air that is sent to the cap, causes the generated droplets to separate from one another. Without the dispersion cap and the dispersion air, monodisperse droplets can coalesce with each other. Also, droplet evaporation is more uniform when drops are made to disperse and separate from one another.

To generate drops using the VOAG, the following procedure is used. First, ballast tank pressure is set to 16 psi by flowing high purity nitrogen to the tank. Second, the 20 μm orifice disk is cleaned with ethanol, dried, and placed in the PZT crystal with the Teflon o-ring placed on top of the disk, as shown in Figure 3-4. Third, the PZT is screwed on to the VOAG head. Fourth, the liquid reservoir is filled with 120 ml of the desired solution to be tested and then the reservoir is connected to the ballast tank. Fifth, the drain tube is opened, followed by the ballast tank being opened. Opening the ballast tank allows the liquid reservoir to pressurize and purges air from the liquid capillary lines. Sixth, once all the air is purged, the drain tube is closed. A liquid stream then flows out of the orifice disk. Flow rate is checked at this time. Seventh, a He-Ne laser is positioned to illuminate the liquid stream. Eighth, with the electrical wiring connected from the frequency synthesizer and square wave generator, frequency and amplitude are programmed into the frequency synthesizer. This causes the PZT crystal to vibrate at the programmed frequency and causes the liquid stream to breakup into droplets. Using the He-Ne laser that illuminates the droplets, a trial-and-error method is used to find the optimum frequency. The optimum frequency is determined when the scattered laser light illuminating the drops is broken up into distinct horizontal lines, which indicates that the droplet stream is highly monodisperse and the drops are spherical. The last step in the

VOAG droplet generation process is to install the dispersion cap and to set the desired flow rate of air to the dispersion cap. With droplets being generated, the settling chamber is put in place and data is collected in a similar fashion to data collection with the UAS. Table 3-1 lists operating parameters for the VOAG experiments.

Table 3-1: Conditions for VOAG droplet testing.

| **Experiment number** | **Solution (mol/L)** | **Orifice (μm)** | **Frequency (kHz)** | **Flow Rate (ml/min)** | **Drop size (μm)** | **Dispersion Cup Flow Rate (ml/min)** |
|---|---|---|---|---|---|---|
| 1 | water | 20 | 110 | .25 | 42 | 1.5 |
| 2 | water | 20 | 110 | .25 | 42 | 1.5 |
| 3 | $10^{-5}$ M $C_8$ | 20 | 100 | .29 | 45 | 1.5 |
| 4 | $10^{-4}$ M $C_8$ | 20 | 100 | .28 | 45 | 1.5 |
| 5 | $10^{-6}$ M $C_8$ | 20 | 120 | .21 | 38 | 1.5 |
| 6 | $10^{-6}$ M $C_8$ | 20 | 110 | .22 | 40 | 1.5 |

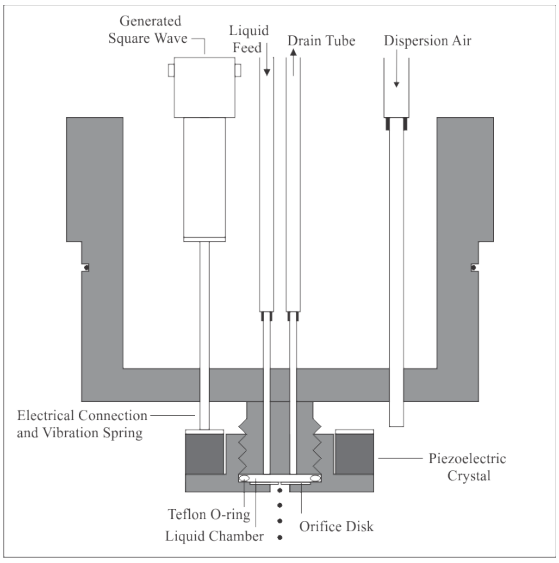


Figure 3-4: The VOAG head without the dispersion cap is shown above. Liquid is sent to the liquid chamber in the piezoelectric crystal via the liquid feed capillary, and then exits the orifice disk. The Teflon o-ring provides a sealed chamber. A drain tube is needed to ensure no air bubbles are in the liquid flow path. The electrical connection transfers the generated square wave to the PZT crystal, which breaks up the liquid stream.

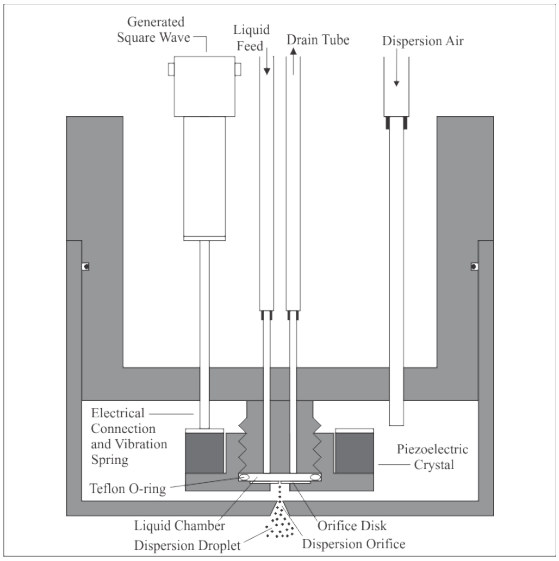


Figure 3-5: The VOAG head with the dispersion cap in place is shown above. The dispersion cap and dispersion air force the generated drops to separate from each other, leading to more uniform evaporation and less droplet coalescence.

## 3.3 Charge Measurement of Droplets

To determine the surface charge of droplets generated in our experiments, two key pieces of information are needed. First, the number of drops in a known volume of the bulk gas is needed. This value is known as the number density. This is determined by the Aerodynamic Particle Sizer 3321, manufactured by Thermo-Systems Instruments. From the Aerodynamic Particle Sizer (APS), the mean diameter of the particles in the volume of bulk gas is also determined. The second key piece of information needed to determine the charges per droplet is the electric current level due to the known amount of droplets hitting the Faraday cup per unit time. This is given by the Aerosol Electrometer 3068B, also from Thermo-Systems Instruments. Both instruments are discussed in the subsequent sections. Using the values of electric current, given by the Aerosol Electrometer (AE), and the values for the number density, given by the APS, we can use the following equation to determine the average number of charges per droplet.

$$\boldsymbol{n_p} = \frac{\boldsymbol{I}}{\boldsymbol{N\ e\ q_e}} \tag{3.3}$$

In 3.3, $n_p$ is the average number of elementary charges per droplet in units of charges per droplet, $I$ is the electric current on the drops (Amperes) and is given by the Electrometer, $N$ is the number density of drops in the bulk gas stream in particles/cm$^3$ and is given by the Aerodynamic Particle Sizer, $e$ is the elementary unit of charge (1.6 x 10$^{-19}$ Coulombs/charge), and $q_e$ is the bulk gas flow rate (cm$^3$/second). Both the electrometer and the APS sampled bulk gas at a rate of 1000 cm$^3$/minute.

### 3.3.1 Aerodynamic Particle Sizer

Droplet number density and droplet mean diameter are properties that allow droplets to be characterized. In our experiments, droplet characterization is performed by an Aerodynamic Particle Sizer (APS) 3321. The APS is a time-of-flight spectrometer that measures the velocity of the droplets as they flow through an accelerating gas. The APS is accurate for droplets in the size range of 0.523 μm to 20 μm diameter, and will determine accurate number densities up to 1000 droplets/$cm^3$. A schematic of the measurement chamber and optics of the APS is shown in Figure 3-6.

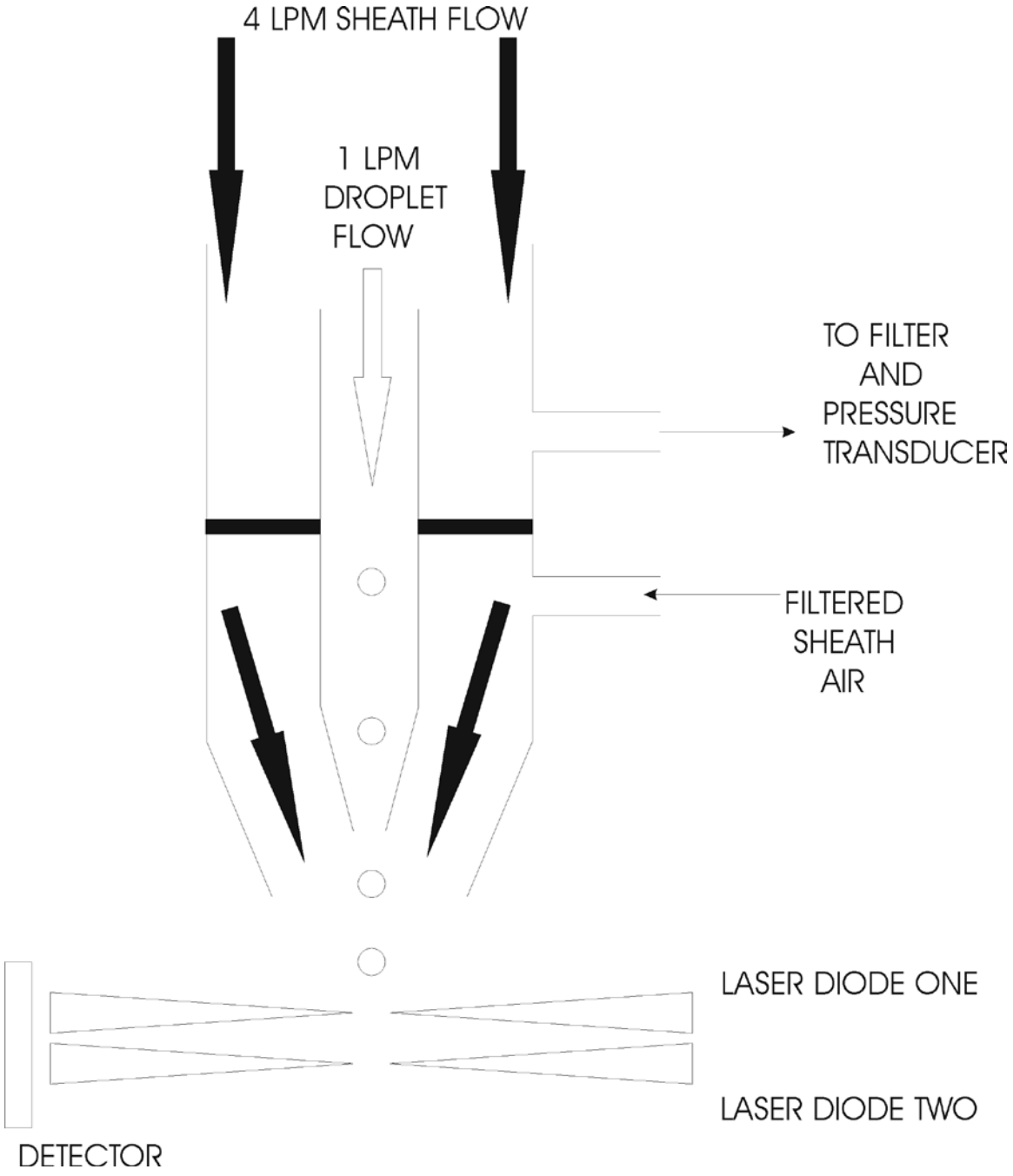


Figure 3-6: Schematic of the Aerodynamic Particle Sizer (APS) 3321. The APS samples 1 liter per minute of droplets (clear arrow), and uses 4 liters per minute of filtered room air (solid arrows) for accelerating the drops through two collimated laser beams. The APS 3321 uses two lasers, which reduces the chances of phantom particles and coincidence error.

The APS pulls droplets into the sampling port at a rate of 1 liter/minute and at the same time the APS also pulls in room air at a rate of 4 liters/minute. The room air is filtered and then is used to accelerate the liquid droplets through a focusing nozzle, and then through two collimated laser beams. The APS 3321 characterizes drops using two lasers spaced closely to each other so the beams overlap. This produces a single, double-crested beam profile if a particle is to be counted. If only one crest is detected, the APS treats the signal as a phantom particle and does not count the particle. If more than two crests are detected, the APS treats this data as coincidence error, and the data is not logged. The APS also uses side-scattering intensity of the laser beams as particles pass through the beams for more accurate droplet size determination.

The Aerodynamic Particle Sizer measures droplet/particle size based on a measurement termed the aerodynamic particle size, which is the diameter of a unit density sphere (specific gravity=1) that has the same terminal settling velocity as the droplet being measured (Hinds 1982). The terminal settling velocity of a droplet is the maximum velocity the droplet will attain in an accelerating flow field, and in our experiments, this velocity is reached in the APS flow nozzle almost instantaneously. For droplets with Reynolds numbers around 1, which applies to our experiments, terminal settling velocity is

$$\boldsymbol{V_{TS}} = \frac{\boldsymbol{\rho_D\, a D_D^2}}{\boldsymbol{18\mu}} \tag{3.4}$$

where $V_{TS}$ is the terminal settling velocity, $\rho_D$ is the density of the settling droplet, $a$ is the acceleration of the flow field, $D_D$ is the droplet diameter, and $\mu$ is the viscosity of the bulk gas the droplet is settling in. As droplets fall in air, or move in a bulk gas, a drag force acts on the droplet causing the droplet to stop accelerating and reach its terminal settling

velocity. The droplet will not speed up or slow down at this point if flow conditions in the bulk gas do not change. The APS measures droplet size by comparing the terminal settling velocity of the droplets to the terminal settling velocity that was calculated for latex spheres that were used to calibrate the instrument. As one can see from 3.4, diameter measurement depends on the density of the droplets of interest compared to the density of the latex spheres. In calibrating the APS, latex spheres of different diameters, all with a specific gravity (SG) of 1.05, are used. After the calibration with latex spheres is performed, a correction factor is programmed into the APS to correct the SG value to that of water, which is 1. At this point, for droplets with SG equal to 1, droplet diameter can be determined by the APS once the APS determines settling velocity using the light scattering technique discussed above.

While water droplets can deform slightly as they are accelerated through the focusing nozzle, the deformation is not significant enough to give measurement error (Baron, 1986). Also, with the overlapping laser beam technology used in the APS 3321, coincidence error like that discussed above in Polat's results is not a factor. Peters and Leith (2003) performed tests with the APS 3321 and found coincidence error of less than 5% in number density over the entire range of the instrument. Finally, TSI used information learned from previous APS models to re-design the APS 3321 circuitry and outer nozzle to eliminate particle re-circulation that previously occurred in the measurement chamber since re-circulation leads to particles being counted more than once.

### 3.3.2 Aerosol Electrometer

The Aerosol Electrometer 3068B is used to measure the electric current due to the charge on a known amount of water droplets. The flow rate into the Aerosol Electrometer (AE) can be varied from 0.3 liters per minute up to 10 liters per minute, and will measure current from particles in the size range of 2 nanometers up to 8 μm. The AE is capable of measuring current values from -12.5 picoamps up to +12.5 picoamps. A schematic showing the operating principle of the AE is shown in Figure 3-7.

The Aerosol Electrometer is a Faraday cup connected to an electrometer. The Faraday cup consists of a highly conductive filter which is mounted in an aluminum housing. As charged particles are drawn into the Faraday cup, they are collected in the filter and the excess charges on the droplets discharge in the filter due to the Faraday Cup being connected to an isolated ground. This generates a flow of charge per unit time, or an electric current. The filter is designed to permanently trap the particles so particle back-scattering does not occur. Back-scattering results in a charged particle being measured more than once.

The amount of current generated due to discharging of the charged particles is measured by the electrometer device of the AE. This device consists of a high-gain amplifier connected to an ammeter. The high-gain amplifier is needed since the electrical current due to the charges on the particles is in the picoampere range. The electrometer flow meter and vacuum pump pull the droplet sample into the AE. For our experiments, flow into the AE was constant at 1 liter per minute.

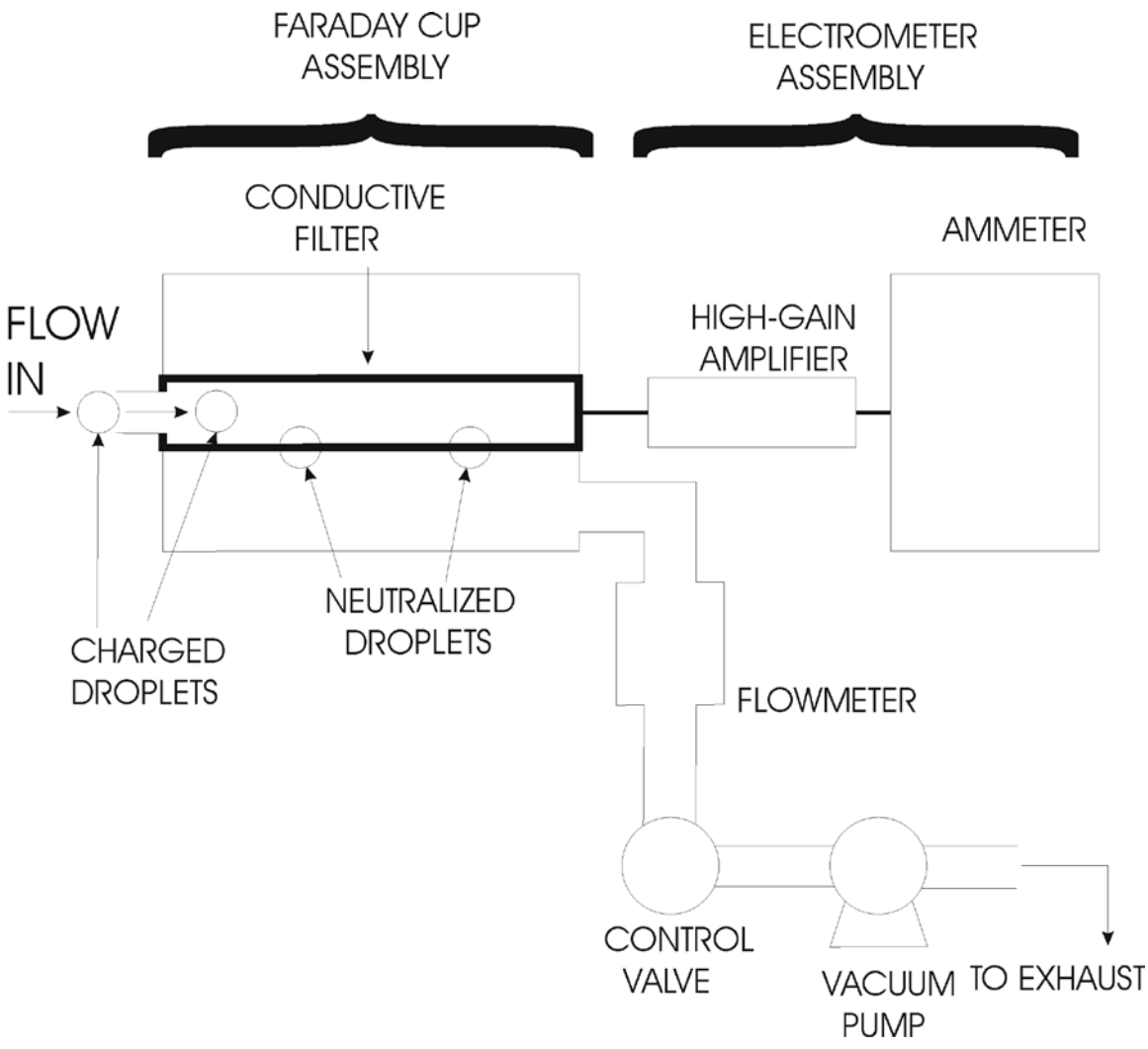


Figure 3-7: Schematic of the Aerosol Electrometer (AE) 3068B. The AE draws charged droplets into the Faraday Cup at 1 liter per minute, and the droplets are collected in the filter, where they discharge. The charge from the now-neutralized droplets is converted to an electrical signal and amplified, and the resultant value is measured by an ammeter and the value then displayed.

## 3.4 Droplet Dispersion System

For valid, reproducible results, generated droplets need to be uniformly dispersed in the settling chamber. This is done by the droplet dispersion system shown in Figure 3-1. The system consists of a rotometer and a vacuum pump. After the sprayer is generating drops and the settling chamber is in place, the droplet dispersion system slowly pulls the droplets down the settling chamber, aiding in getting droplets to the APS and AE for sampling. This system is needed since droplets in the size range we are dealing with will settle in air and fall at a very slow rate. For instance, a 5 μm droplet will fall in still air at 4.5 meters per minute. At this rate, considerable evaporation has taken place by the time the droplet enters the sampling port for the APS and AE. The dispersion system speeds up this process. Flow rates of 5 liters/minute to 10 liters/minute were used to disperse droplets.

## 3.5 Experimental Procedure

In order to perform experiments and produce data, the droplet generators must be generating spray droplets. In Sections 3.2.1 and 3.2.2, the procedure for starting and operating the Ultrasonic Atomizing Sprayer and the Vibrating Orifice Aerosol Generator is discussed. The experimental procedure for testing the surface charge on droplets after the droplet generators are running properly is now covered.

Once droplets are being generated, the settling chamber is put into place as shown in Figure 3-1. After the settling chamber is in place, the vacuum pump for droplet dispersion is turned on and the flow rate is set. Drops are sprayed into the chamber for 10 minutes to allow the chamber to reach 100% relative humidity, which leads to uniform evaporation of the droplets entering the chamber. This also minimizes static charges on the chamber walls. After this 10 minute period, the Aerodynamic Particle Sizer (APS) is connected to the sampling port on the side of the settling chamber. Figure 3-1 shows both the AE and the APS connected to the settling chamber, but in reality only one instrument is connected at a time. Figure 3-1 was drawn to give the reader a clear idea of the experiment. By sampling with the APS and the AE from the same port, we found the results to be more reproducible. The sampling procedure is discussed in further detail in Chapter 4 on Analysis of Raw Data, but a summary is given below.

Droplet samples are drawn into the APS at a rate of 1 liter per minute and the sample is monitored and data recorded for 55 seconds. The data from this 55 second sample is averaged over the 55 seconds and then summarized and represents one sample. After the 55 second sample, the number density and the mean droplet diameter are calculated for that 55 second sample. The APS is programmed not to monitor the sample for the next 5

seconds, and then begins monitoring for another 55 second. Steady state is achieved once the drops are not changing in diameter or number density. When this occurs for at least three samples in a row, the number density and the mean diameter values are recorded and the APS is removed from the settling chamber. The Aerosol Electrometer (AE) is now connected to the same sample port. The AE draws droplet samples into the unit at 1 liter per minute, which is the same sampling rate as the APS. Once charged droplets begin to dissipate their charge to the conductive AE filter, an electrical current flows and the value is displayed. Samples of four minutes are taken with the AE and data is considered valid when all data is within three standard deviations of the mean electrical current value. When the current has reached steady state, the value is recorded and the AE is disconnected from the sample port, and the APS is re-connected to the sample port. Samples of 55 seconds are again taken with the APS. If the number density and mean drop diameter are consistent compared to the data from before sampling with the AE, then the values of electrical current, drop number density, and drop diameter are determined to be accurate and one full charge measurement sample has been taken. Using 3.3, the charge per droplet can now be calculated.

It should be noted that conductive carbon-impregnated tubing is used for droplet sampling into both the APS and the AE. Polyethylene and PVC tubing can act as insulators and charged droplets that hit the inside tubing wall will stay in place while retaining their charge, which can skew results.

## 3.6 Preparation of Ionic Surfactant Solutions

Four different surfactants were used in this study. Figure 3-8 shows the molecular structure of the surfactants. The anionic surfactants differed only in hydrocarbon chain length. Table 3-2 lists additional information on the surfactants used.

Surfactant solutions were prepared by mixing one master solution for each of the surfactants tested, and then the differing concentrations for the particular surfactant were mixed from those master solutions. This needed to be done since concentrations tested were mostly $1 \times 10^{-4}$ M through $1 \times 10^{-6}$ M and accurate measurements of solutions in the quantity range we were using was highly inaccurate.

Once solutions were mixed, the solution was drawn into the syringes (for the UAS tests). The syringes were allowed to sit overnight oriented so any air bubbles formed would rise to the top of the syringe and could be easily purged. For VOAG testing, the liquid reservoir was filled the night before testing so air bubbles could again rise to the top of the reservoir and not get in the liquid lines to the VOAG.

Nitrile gloves were worn when any part of the liquid system was handled since even a slight amount of oil from one's skin is in itself a surfactant and can adversely affect results since we are dealing with such low surfactant concentrations.

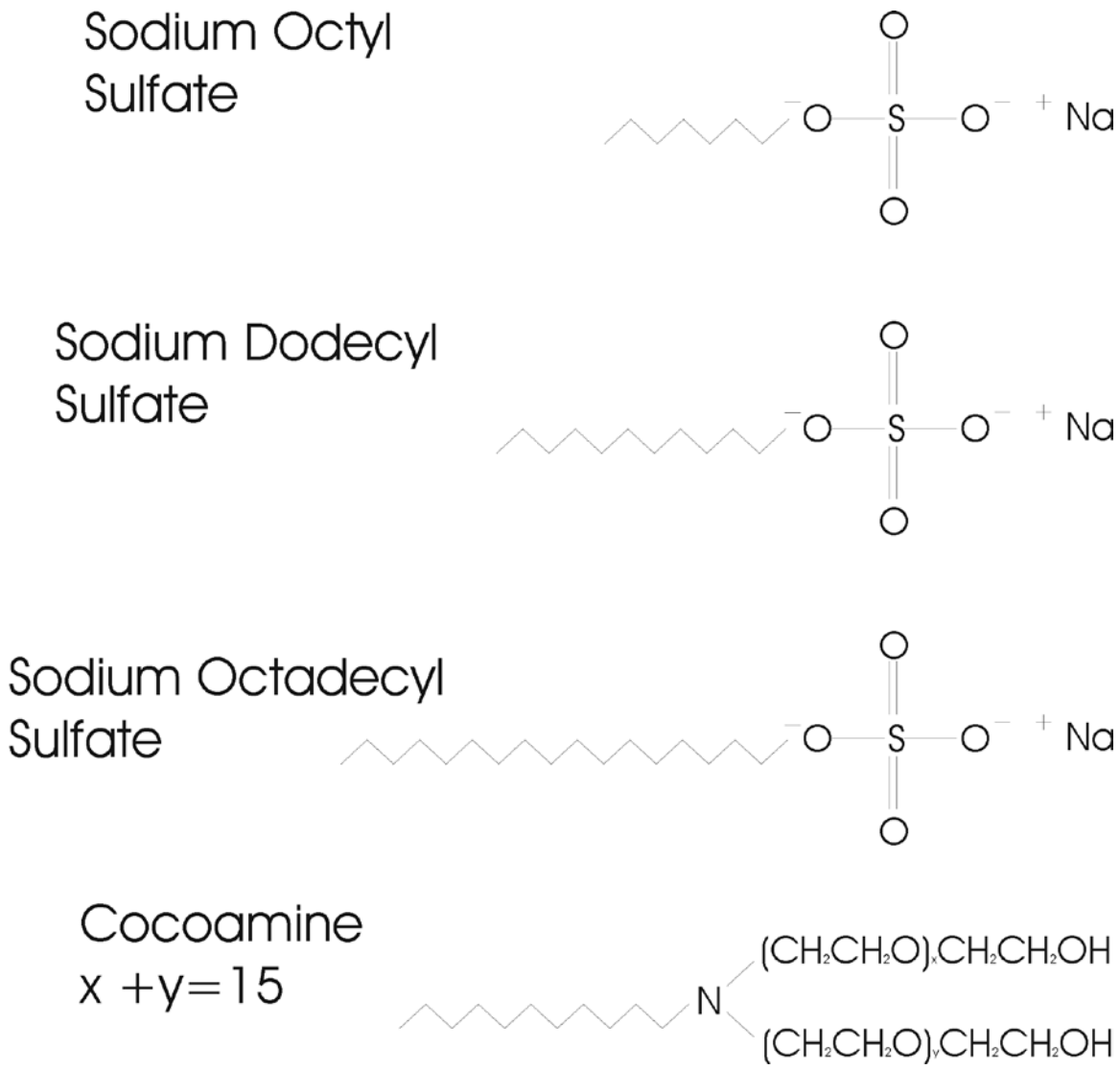


Figure 3-8: Structures of the four surfactants used in charge measurement experiments. For the cocoamine, “x” plus “y” represent the number of the ethylene oxide groups and totaled 15 for the cocoamine used in the experiments.

Table 3-2: Properties of four surfactants used in the experiments.

| Surfactant | Molecular weight | Type (anionic or cationic) | Structure (straight-chain or branched) | Formula |
|---|---|---|---|---|
| Sodium Octyl Sulfate | 232 | Anionic | Straight | $NaC_8H_{17}SO_4$ |
| Sodium Dodecyl Sulfate | 288 | Anionic | Straight | $NaC_{12}H_{25}SO_4$ |
| Sodium Octadecyl Sulfate | 373 | Anionic | Straight | $NaC_{18}H_{37}SO_4$ |
| Polyethoxylated Tallow Amine | 825 | Cationic | Branched | $C_{16}H_{35}O_2N(C_2H_4O)_x(C_2H_4O)_y$ |

# Chapter 4
# Analysis of Raw Data

## 4.1 Introduction

For measurement of excess surface charges per droplet, an accurate measurement of current generated by the droplets, as well as droplet characterization, is needed. The measurement concepts of drop characterization with the Aerodynamic Particle Sizer (APS) and drop current measurement with the Aerosol Electrometer (AE) were discussed in Chapter 3. Chapter 4 discussed how raw data was analyzed.

At this time, recall that surface charge per droplet is calculated by Equation 3.3,

$$\boldsymbol{n_p} = \frac{\boldsymbol{I}}{\boldsymbol{N\, e\, q_e}} \tag{3.3}$$

where $n_p$ is the average number of elementary charges per droplet in units of charges/droplet, $I$ is the electric current on the drops (Amperes) and is given by the Electrometer, $N$ is the number density of drops in the bulk gas stream in particles/cm$^3$ and is given by the Aerodynamic Particle Sizer, $e$ is the elementary unit of charge ($1.6 \times 10^{-19}$ Coulombs/charge), and $q_e$ is the bulk gas flow rate (cm$^3$/second). This equation is presented again as a reminder that to calculate excess surface charges per droplet, the number density of droplets ($N$) is needed, and the current generated from a droplet sample ($I$) is needed.

For the data analysis that will ultimately give values for $N$ and $I$, we interface the APS and the AE with a Dell Inspiron computer with a Windows XP operating system running the Aerosol Instrument Manager (AIM) software from Thermo-Systems Instruments. How data is analyzed by the AIM software from the APS and AE is presented in Sections 4.2 for the droplet characterization, and in Section 4.3 for the droplet current. Section 4.4

discusses the difference between droplets generated by the UAS compared to the VOAG. The UAS generates a polydisperse stream of droplets and the VOAG generates a monodisperse stream of droplets.

## 4.2 Determination of droplet size and number density

The Aerodynamic Particle Sizer (APS) is used to determine the number density, which is the number of drops per unit volume, as well as the droplet diameter. We interface the APS with the AIM software and the useful results are displayed in the form of a histogram and a statistics summary table. Figure 4-1 shows the histogram and Figure 4-2 shows the statistics summary table.

The APS is programmed to monitor the diameter distribution of the droplet sample and the droplet number density for 55 seconds, then wait 5 seconds, then monitor another 55 second sample. This continues during the entire time that droplets are being drawn in to the APS. At the end of each 55 second sample, the values are averaged over the 55 seconds and the histogram and statistics summary table (SST) are displayed with summary data for the 55 seconds. These averaged values for mean droplet diameter, shown in bold type in the SST of Figure 4-2, and the number density, shown in bold type in the SST of Figure 4-2, now represent the drop characteristics for the entire 55 second sample and are now considered a single sample. The 55 second droplet sampling procedure continues until the system is at steady state, which we have determined occurs when the histograms from each single 55 second sample look very similar from one sample to the next, and when mean diameter and number density values in the SST are within 3% of each other. Once steady state is attained, three more samples are taken. We

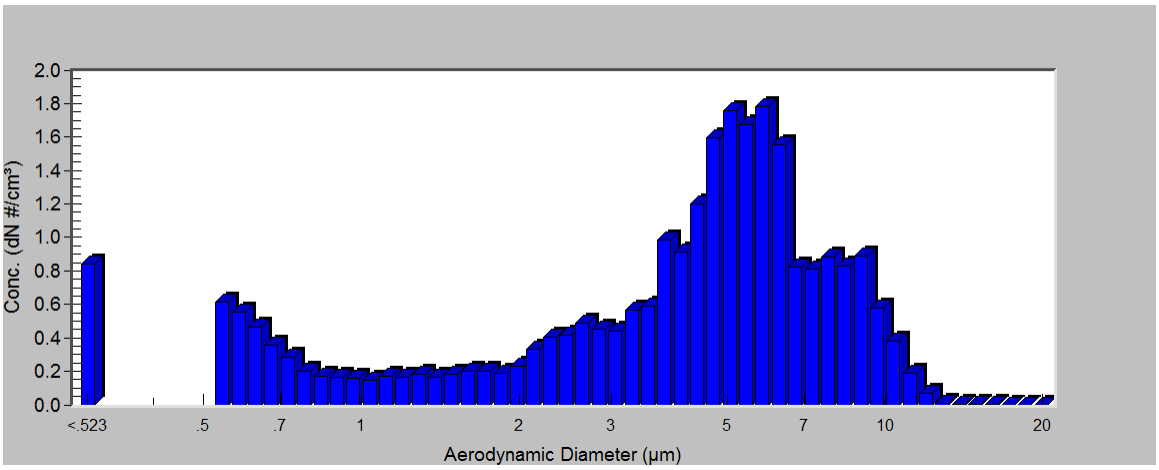


Figure 4-1: The droplet size is shown as a histogram that graphs number of droplets versus droplet size. The data is generated by the APS and processed by the AIM software.

Table 4-1: Statistics Summary table generated by the APS.

| | **Number** |
|---|---|
| | **Particle Size** |
| **Median (µm)** | **4.77** |
| **Mean (µm)** | **4.69** |
| **Geo. Mean (µm)** | **3.71** |
| **Mode (µm)** | **5.83** |
| **Geo. St. Dev.** | **2.21** |
| **Total Conc.** | **32.1(#/cm³)** |

now take the mean droplet size and number density from the three steady state samples and average them, with the resultant number density being used in Equation 3.3 for the variable *N*. The averaged value of the three samples for mean droplet diameter is used when analyzing and graphing excess surface charges per droplet versus droplet diameter. After sampling is performed with the Aerosol Electrometer, the APS is again connected to the settling chamber to determine if the droplet stream is still showing the same droplet size and number density. If it is then we conclude that we are still at steady state and our data from that sample is valid.

## 4.3 Current Generated from Droplets

The current generated from droplets impacting the Faraday Cup in the Aerosol Electrometer (AE) is measured as the current is discharged and the data is analyzed and reduced with the AIM software. In the above section, the method for determining if the droplet measurement system is at steady state is discussed. Once the system is at steady state and droplet characterization data has been calculated, the APS is disconnected from the droplet sampling port and the AE is connected. At this point, the AIM software is prompted to begin recording the data signal from the AE. Data from the AE is recorded for 4 minutes and the software generates the graph shown in Figure 4-2 in real time. After four minutes of sampling time, the AIM software is prompted to end data collection from the AE. The software then calculates the mean current generated by the drops for the four minute sample, as well as the standard deviation of the four minute sample. If all the data lies within 3 standard deviations of the mean, the numbers are accepted as valid. The average current value is now recorded as the variable $I$ in Equation 3.3. With the value of current ($I$) now known, and the value for number density ($N$) known from the APS, we can calculate the value for the number of excess surface charges per droplet.

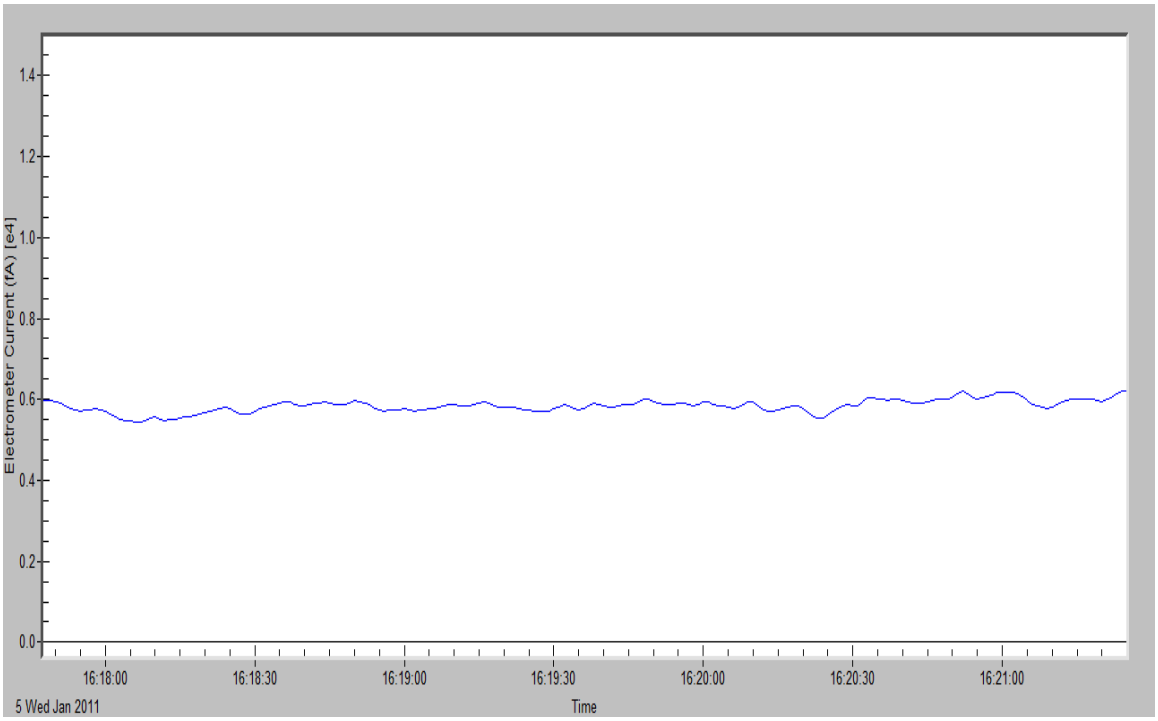


Figure 4-2: The AIM software reduces data from the AE then graphs Electrometer Current versus time. The graph is generated in real time so trends are seen immediately.

## 4.4 Droplet Diameter Histograms from the UAS and the VOAG

As stated previously, the Ultrasonic Atomizing Sprayer (UAS) generates a polydisperse stream of droplets, and the Vibrating Orifice Aerosol Generator (VOAG) generates a monodisperse stream of droplets. To gain a better understanding of these terms, see the histograms presented in Figure 4-3 and Figure 4-4.

Figure 4-3 shows the polydisperse distribution of droplet diameters for droplets generated by the UAS. The histogram for the UAS shows a wide distribution of droplet diameters and there are two peaks in diameter, the first around 0.55 μm in diameter, and the second around 6 μm in diameter. The peak at the far left of the histogram for diameters <0.523 μm can be disregarded because the APS cannot accurately characterize droplets with diameters smaller than 0.523 μm. Due to the polydisperse distribution of droplets generated by the UAS, many more experiments had to be performed before definite trends were seen in our data. Polydisperse droplet generation is the key negative point of the UAS since much more data is needed before trends are seen. The key positive to the UAS is it is easier to operate, compared to the VOAG.

Figure 4-4 shows the monodisperse distribution of droplet diameters for droplets generated by the VOAG. The histogram for the VOAG shows a narrow distribution of droplet diameters, with only one peak around 0.55 μm in diameter. Again, the peak at <0.523 μm can be disregarded because the APS cannot accurately characterize droplets with diameters smaller than 0.523 μm. The key advantage to droplet generation with the VOAG is the monodisperse distribution of droplets seen in the histogram of Figure 4-4. Only a limited number of experiments need to be performed with the VOAG before

definite trends are seen in the data. The drawback to the VOAG is that it is sometimes difficult to operate.

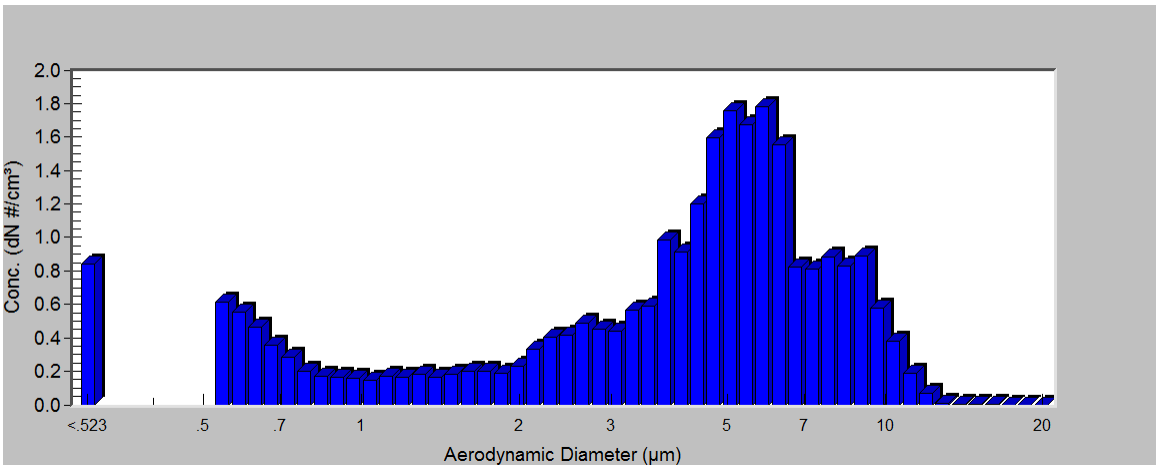


Figure 4-3: A histogram for droplets generated by the UAS shows a wide distribution of droplet diameters, and two peaks for diameter. The single line shown at the far left of the histogram can be disregarded.

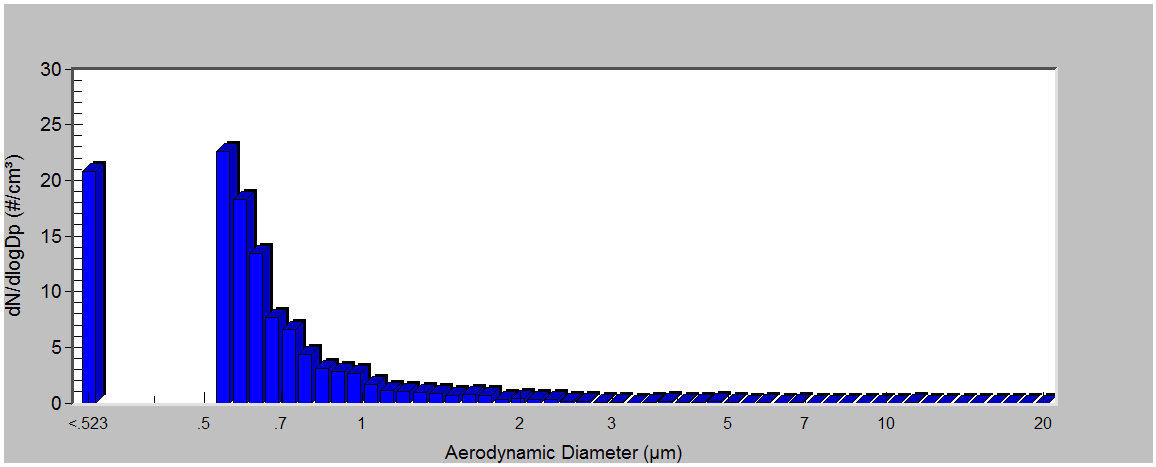


Figure 4-4: A histogram for the droplets generated by the VOAG shows a narrow distribution of droplet diameters, and only one peak, seen at 0.55 µm in diameter. The single line shown at the far left of the histogram can be disregarded.

# Chapter 5
# Results and Discussion

## 5.1 Introduction

As mentioned previously, two sprayers were used in this study, and four different surfactants were tested, with the objective of determining if ionic surfactants can modify and enhance the amount of charges on the surface of water droplets. During the course of this study we also learned that the rate of liquid break-up/droplet generation will determine droplet polarity. Previous investigators showed that surface charge on surfactant solution droplets is influenced by ion diffusivity through the bulk droplet to the surface, the number of surfactant ions per unit of surface area, and the depth of the charge at the surface.

Chapter 5 is organized as follows. Section 5.2 presents data from the Ultrasonic Atomizing Sprayer (UAS). Section 5.2.1 shows data for water droplets generated by the UAS. Section 5.2.2 shows data comparing aqueous cocoamine and sodium dodecyl sulfate (SDS) droplets generated by the UAS. Section 5.2.3 shows UAS data for SDS in which droplet charge versus SDS concentration is presented. Section 5.2.4 shows UAS data for a comparison of the droplet charge generated from the three anionic surfactant solutions at concentrations of $5.4 \times 10^{-5}$ M. Section 5.2.5 shows data from water and the three anionic surfactants in which UAS power level used to generate drops was altered. Section 5.3 shows data for droplet charge where droplets were generated by the Vibrating Orifice Aerosol Generator. Section 5.4 discusses the results shown in the data.

## 5.2 Charge of droplets generated by Ultrasonic Atomizing Sprayer (UAS)

The objective of this study is to determine whether the addition of ionic surfactants to water droplets can enhance the surface charge of spray droplets. To meet our objective, pure water droplets must first be tested to establish a baseline level for charges per droplet, denoted as $Q_D$. Using this baseline number for charge per water droplet, a comparison can be made to droplets generated from surfactant solutions.

As discussed before, droplet charge was measured by spraying droplets from the Ultrasonic Atomizing Sprayer (UAS) into the settling chamber, then using the droplet dispersion system to disperse the drops uniformly through the settling chamber. Once this was done, the Aerodynamic Particle Sizer and the Aerosol Electrometer were used to determine droplet diameter, droplet number density, and the number of charges on the droplet surface.

Experiments with deionized water droplets were done first and the results are presented now in Section 5.2.1. Followed Section 5.2.1, droplet data from additive solutions is presented in the subsequent sections. All data presented in Section 5.2 is from experiments with the Ultrasonic Atomizing Sprayer.

### 5.2.1 Surface charge on water droplets from the UAS

In our experiments on water droplets generated with the UAS, drops were generated at two different sprayer power levels. Most experiments were done with a sprayer power level of 6.8 W, but data with a power setting of 3.7 W were also generated.

Figure 5-1 and 5-2 show data for water droplets that were produced at a sprayer power level of 6.8 W. In section 5.2.5, data from droplets generated with the UAS with a power setting of 3.7 W are discussed.

Figure 5-1 shows how charge per droplet increases as droplet size increases and the data fits a power law model, shown as Equation 5.1.

$$\boldsymbol{Q_D = 722.96 D_D^{0.3652}} \quad (5.1)$$

In Equation 5.1, $Q_D$ is charge per droplet, and $D_D$ is droplet diameter. In general, charge per droplet should fit a power law model with an exponent less than one since an asymptotic relationship is expected. As droplet size gets bigger, charge per droplet cannot not go to infinity, so it is expected that charge per droplet should eventually reach a constant level.

Figure 5-2 compares data presented in Figure 5-1, with data from Blanchard (1958), Polat et al. (2000), and Zilch et al. (2008) included in the graph. The data in Figure 5-2 fits a power law model with an exponent less than one, which is what one would expect. The results from other investigators are shown in Figure 5-2, but all data in Figure 5-2 are fitted to Equation 5-2 for comparison.

$$\boldsymbol{Q_D = 628.04 D_D^{0.462}} \quad (5.2)$$

Equation 5-2 will not be used for data analysis in this study. It is only shown to convince the reader and ourselves that our experimental design will generate plausible results. We

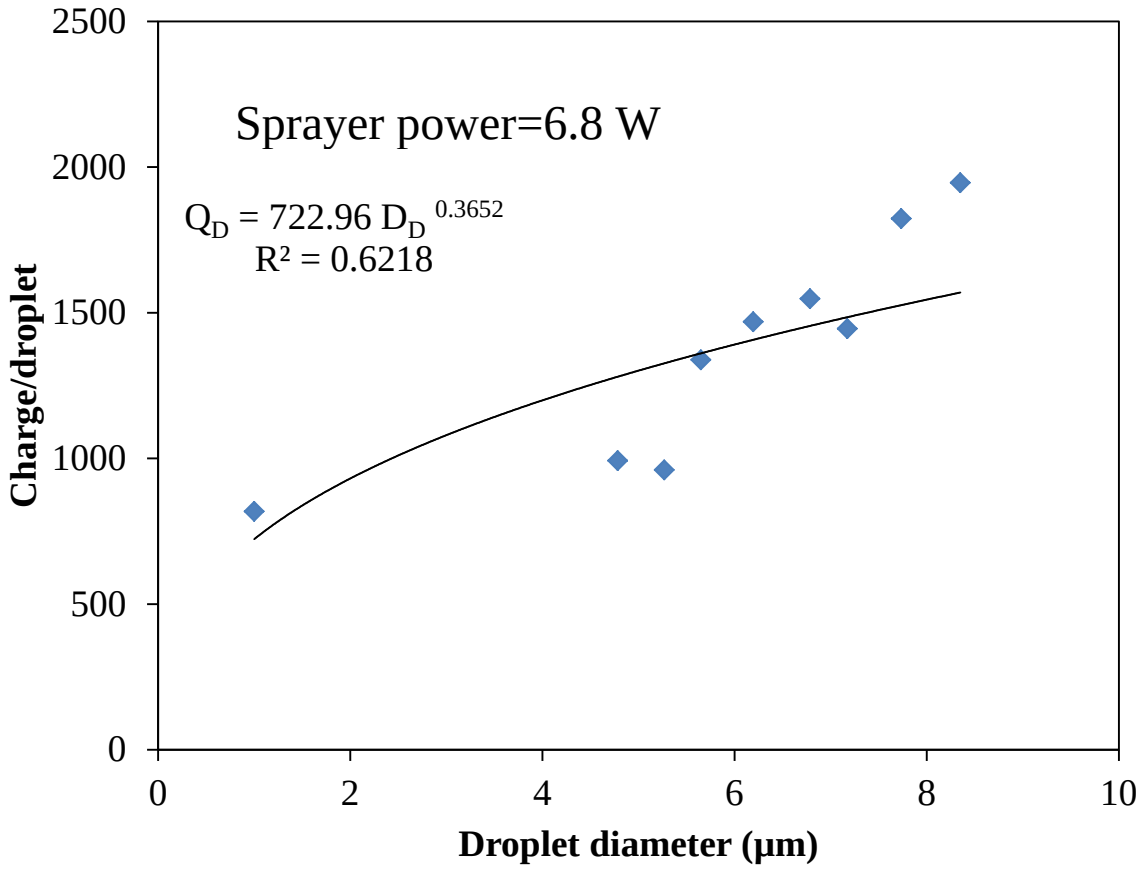


Figure 5-1: Charge per water droplet data from the Ultrasonic Atomizing Sprayer (UAS). As droplet diameter increases, charge per droplet increases.

will use Equation 5-1 when comparing results for surfactant solution droplets versus water droplets. A comparison of this type will allow us to quantitatively judge if an aqueous surfactant droplet has more surface charge than a pure water droplet.

As seen in Figure 5-1 and 5-2, water droplets that we generated were less than 10 μm in diameter. As reported in the literature, once droplets get larger than about 10 μm in diameter, inertial forces begin to influence particle motion and coulombic forces govern particle motion less and less. In our experiments, we sought to investigate electrostatic/coulombic properties of droplets. For this reason, we generated droplets with mean diameters of about 5 μm.

All water droplets generated with the UAS at a power level of 6.8 Watts had an excess of positive charges. This occurred because at a power level of 6.8 W, the electrical double layer (EDL) does not have time to re-establish itself before a new droplet is being formed. This concept was discussed in detail in Chapter 2 and will be revisited in the Section 5.4.

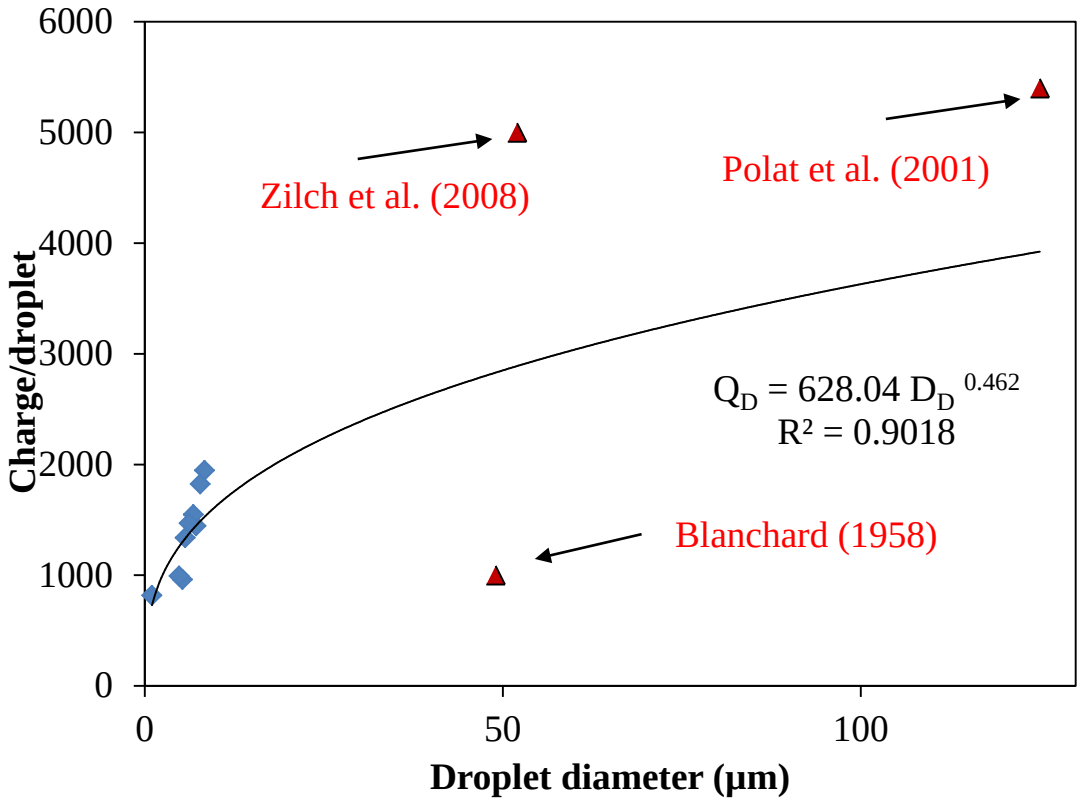


Figure 5-2: Our water droplet data from the Ultrasonic Atomizing Sprayer (UAS), with data from other investigators included. Data from our experimental system is in line with data presented by other investigators.

### 5.2.2 Surface charge comparison on aqueous cocoamine and sodium dodecyl sulfate droplets from the UAS

After a baseline charge level for water droplets was determined in our experiments, we tested droplets with surfactant additives. Figures 5-3 and 5-4 show our results for cocoamine (CAM) and sodium dodecyl sulfate (SDS) droplets, which were the first two surfactants tested in our additive experiments. An introduction to CAM and SDS is given above in the experimental section, but the key feature of the two surfactants is that CAM is a branched molecule and SDS is a straight-chained molecule. Two CAM concentrations were tested and one SDS concentration was tested. The CAM concentrations were $1 \times 10^{-6}$ M and $2.36 \times 10^{-6}$ M and the concentration of SDS was $5.4 \times 10^{-5}$ M. The power to the sprayer was maintained at 6.8 W during these experiments. The CAM data are presented in Figure 5-3, and the water droplet results are shown for comparison.

Figure 5-3 shows that a charge enhancement is seen with CAM solutions. For instance, when comparing 6 μm droplets, water showed a charge of ~1500 charges per drop, but the CAM droplets showed 5000 charges per drop, which corresponds to and enhancement of over 300%.

Figure 5-4 compares droplet charge results for CAM and sodium dodecyl sulfate (SDS), allowing us to learn more about the first objective of this thesis. Recall that the first objective in this study is to determine if the number of surfactant ions per unit of surface area has an influence on droplet charge. Several investigators cited in this thesis report that steric hinderances at the droplet's air/water interface play a role in determining the number of excess charges on a droplet surface. CAM is a more bulky molecule compared

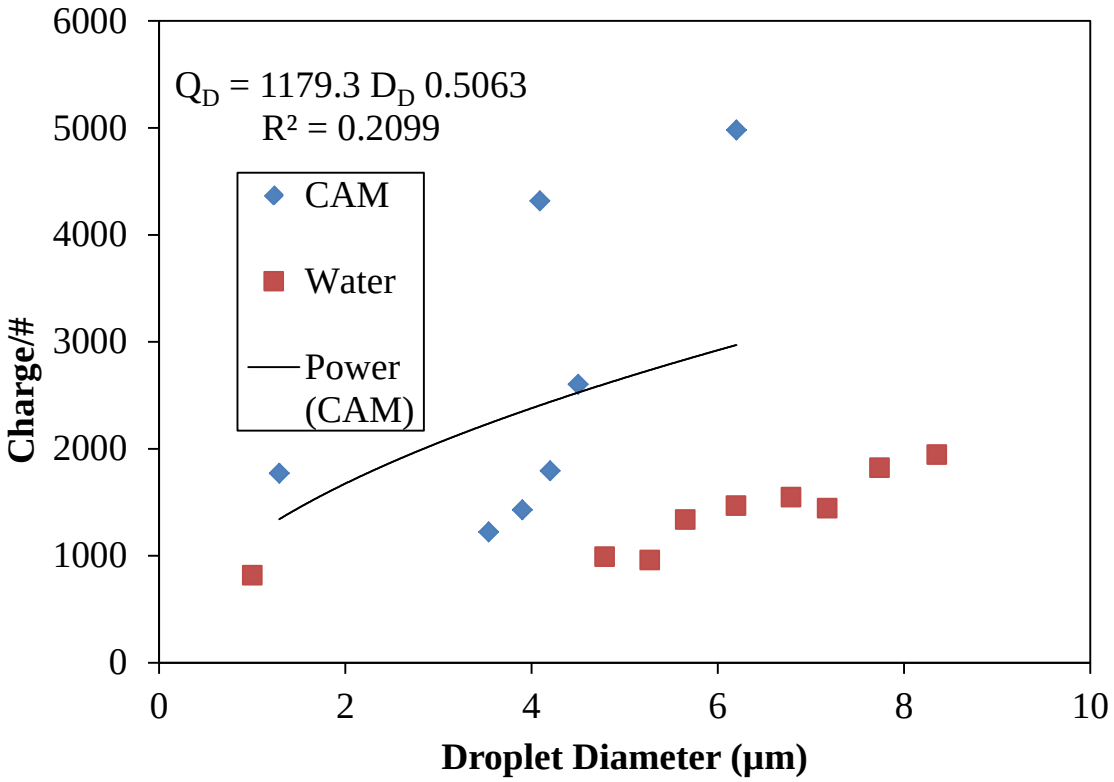


Figure 5-3: Aqueous solutions of cocoamine (CAM) were used to generate droplets and the results are presented here. Water droplet data are presented as well for reference.

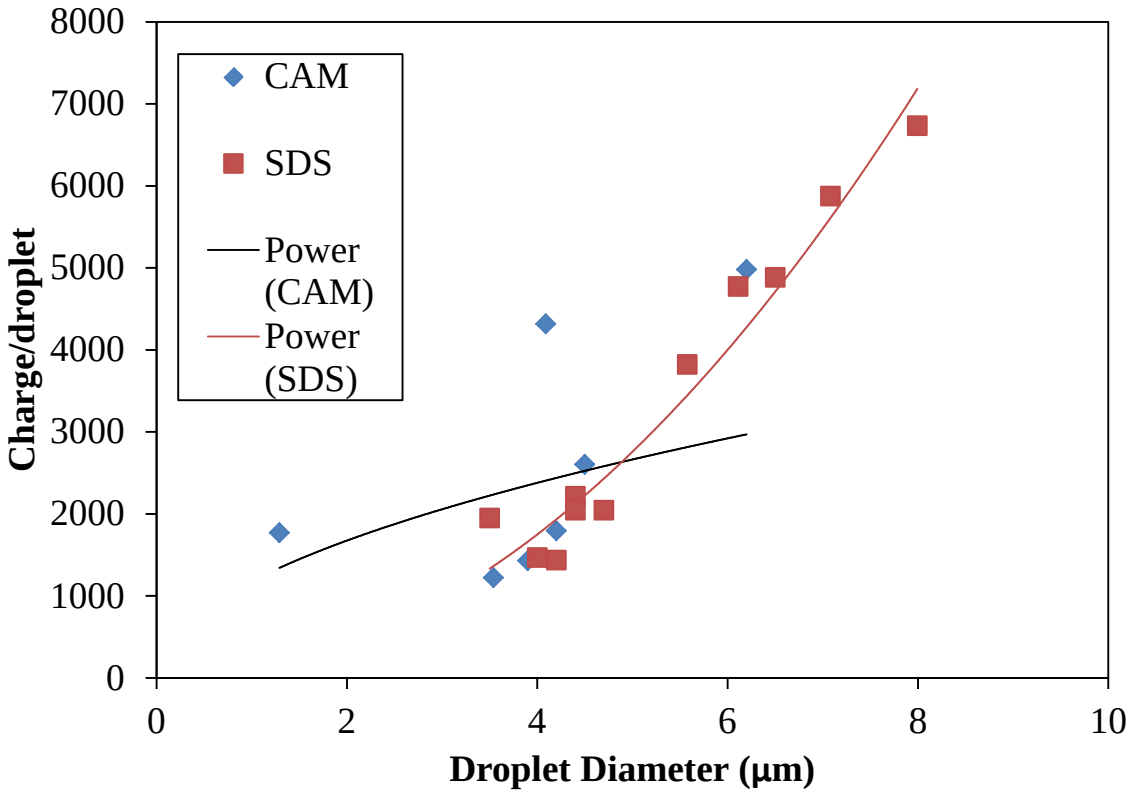


Figure 5-4: A comparison of charge per droplet versus droplet diameter is shown for SDS and CAM droplets. It cannot be determined if one surfactant enhances charge more than the other.

to SDS. Unfortunately, it cannot be determined which surfactant enhances charge to the greatest extent, since, as shown in Figure 5-4, both enhance droplet charge. If the power law model is valid as drawn on the plot, the SDS could be judged as the better surfactant for droplet charge enhancement. In retrospect, these two molecules were not good for side by side comparison for objective one. They are very different in structure and one is anionic and one is cationic. Future work to validate objective number one should focus on two similar molecules, differing only by branched and straight chain hydrophobic groups.

The CAM tests also lacked reproducibility in the results. The explanation for this is that during testing, the sprayer and liquid supply lines could not be cleaned well enough between runs so that we could be assured that no CAM residue was left in the system. This would cause air bubbles in our liquid lines which altered liquid flow rates. Experience taught us that experimental results were generally poor if liquid flow could not be precisely controlled. Also, at the low level of surfactant concentrations we were dealing with, even residue left in the liquid lines could alter the concentration in the drops being generated. To get our experimental system completely clean and free of CAM residue, a time consuming disassembly process had to be performed on the sprayer system. At this point we decided to remove CAM experiments from our test matrix. In the future, more work with CAM should be performed since CAM did enhance drop charge to a great extent.

### 5.2.3 Aqueous Sodium Dodecyl Sulfate Droplet Charge Versus Concentration from the UAS

As discussed above in Section 2.5, droplet charge testing by Matteson (1971), Polat et al. (2000), and Chein et al. (2004) showed that sodium dodecyl sulfate (SDS) enhanced droplet charge the most of any of the anionic surfactants tested. We wanted to repeat their respective studies because in our experiments we use an Aerodynamic Particle Sizer (APS) to determine droplets diameter and droplet number density and an Aerosol Electrometer to test current generated by droplets. The other investigators mention before used less accurate methods for testing. Polat et al. used a camera with a telescopic lens to characterize drops, which is not as accurate as our APS. The apparatus used by Chein et al. for measuring current generated by droplets was to catch droplets on a metal screen and measure current from the drops with an ammeter. The Aerosol Electrometer we used is much more accurate. In Matteson's work, he did not directly measure droplet diameters or droplet density, choosing instead to make educated guesses about drop characterization.

Charge per droplet data was generated using different concentrations of SDS using the Ultrasonic Atomizing Sprayer (UAS) with a sprayer power setting of 6.8 W, and the results are shown in Figure 5-5. The SDS concentrations used were $1.0 \times 10^{-6}$ M, $2.5 \times 10^{-6}$ M, $3.1 \times 10^{-6}$ M, $2.0 \times 10^{-5}$ M, $5.4 \times 10^{-5}$ M, and $6.4 \times 10^{-5}$ M. The results are shown in Figure 5-5 using data for SDS drops of 4 µm through 5.9 µm, drops of 6 µm, and drops of 7µm. When comparing this data with that of water shown in Figure 5-1, a charge enhancement can be seen. Enhancement is higher for droplets with an SDS concentration of $5.4 \times 10^{-5}$ M, which is similar to what Polat et. al. observed.

Section 2.5 also discussed how concentration plays a key role in determining the magnitude of charge enhancement of spray droplets. Polat et al. observed the greatest charge enhancement with solutions of $5 \times 10^{-5}$ M SDS, Matteson observed the greatest charge enhancement with solutions of $5 \times 10^{-5}$ M SDS, and Chein et al. showed the greatest charge enhancement with solutions of $1 \times 10^{-4}$ M SDS. We wanted to test charge per droplet versus concentration for SDS solutions using our instrumentation to see how our results compare.

While the experimental results presented in this section do little to meet the three objectives of this thesis, knowledge of the maximum charge per droplet is needed if Equation 2.4 and 2.5 are to be optimized. The reader must keep in mind that we are looking to find ways to generate spray droplets with the highest level of surface charge possible, and the results presented here are intended to do that.

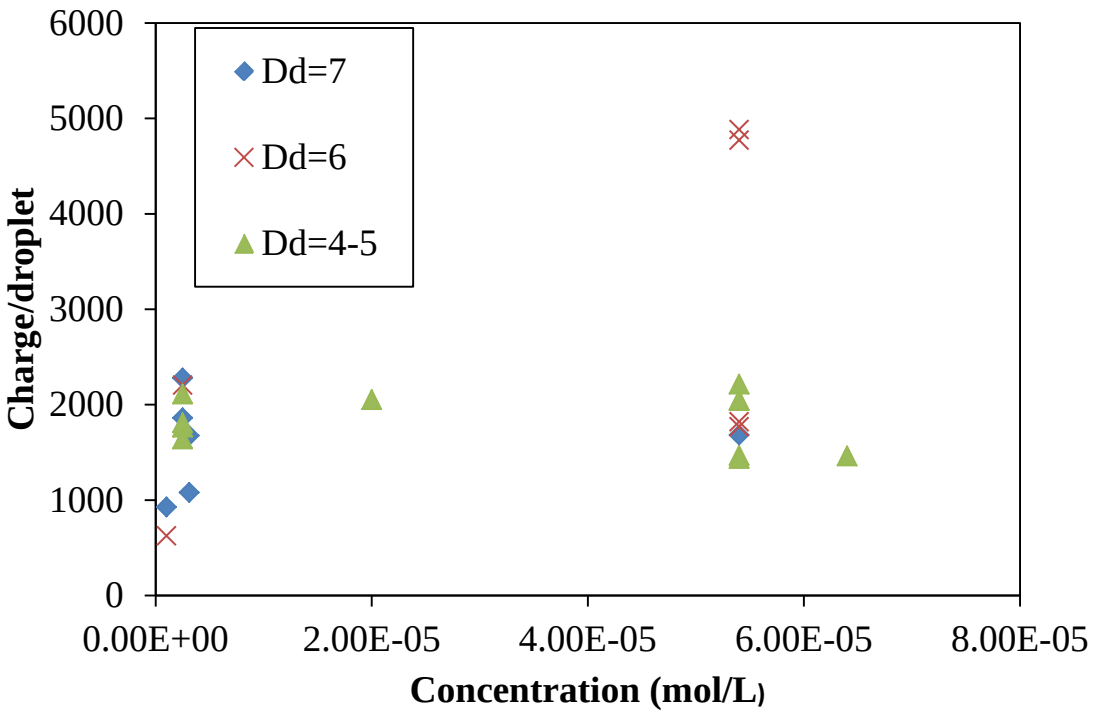


Figure 5-5: The results are for drops generated with six different concentrations of SDS solutions, grouped by three different droplet diameters.

## 5.2.4 Surface Charge Comparison for Three Anionic Surfactants from the UAS

The second and third objectives of this study were to investigate whether molecular chain length affects charge per droplet. Molecular chain length affects the diffusion rates of the molecules in the liquid droplet, and chain length also affects the depth at which droplet charge lies. We chose to test three anionic surfactants that differed only in chain length of the hydrophobe, and the results are presented in Figure 5-6.

In recalling the work of Iribarne and Mason (1967), they derived an equation, shown as Equation 2.7, in which they theorized that molecular chain length was inversely proportional to droplet charge. In Section 2.5, Matteson is cited due to his theory that surfactant diffusion to the droplet surface is the key factor in charge enhancement. To test these theories, three anionic surfactants were selected that differed only in the length of the hydrocarbon chain. The structures were presented above in Figure 3-7. All three molecules had a sulfate functional group as the hydrophilic end of the molecule, and the hydrophobic ends differed only in the lengths of the normal hydrocarbon chain. The sodium octyl sulfate (SOS) has an eight member hydrocarbon chain, the sodium dodecyl sulfate (SDS) has a twelve member hydrocarbon chain, and the sodium octadecyl sulfate (SODS) has an eighteen member hydrocarbon chain. All three anionic surfactants had normal hydrocarbon chains, with no branching in the hydrophobic end, and sodium was the counter ion in all three surfactants. The work of Iribarne and Mason was one of the reasons for selecting these surfactants since, again, they theorized that shorter chain lengths lead to higher droplet charge. The second reason for selecting these surfactants was based on work by Varadaraj et al. (1992). He performed experiments testing surface tension of straight chain SDS versus branched-chain SDS and found straight-chained

SDS lowered the surface tension of water-based solutions more than the branched SDS. Varadaraj et al. theorized that the lower surface tension of the n-SDS molecule in solution was due to the fact that n-SDS could more densely pack the water surface at the air/water interface. In our case, this amount of surfactant packing at the surface could lead to a higher surface charge, therefore we chose straight-chained surfactants for testing.

Since charge enhancement was seen with $5.4 \times 10^{-5}$ M SDS solutions in our results and the results presented in the literature, we decided to test SOS and SODS at concentrations of $5.4 \times 10^{-5}$ M. The results are presented in Figure 5-6, along with water data for reference purposes. One immediately notices that charge is enhanced with all three surfactants, but the greatest charge enhancement seen was with the SOS surfactant, which is the shortest of the three anionic surfactant molecules tested. A line is drawn through the data for the SOS molecule. Based on our experimental results, it would appear that a shorter chained molecule will enhance surface charge to the greatest extent. What is not known is which theory, Iribarne and Mason's, or Matteson's can be used to explain the results. SOS is the shortest molecule tested, so it will diffuse to the droplet surface the fastest, as Matteson would suggest. Iribarne and Mason's work would suggest that the relatively short length of SOS will maximize the mass balance of surfactant ions at the surface. Future work in this area is needed to determine if SOS shows the greatest charge enhancement due to faster diffusion, or if it is due to the mass balance at the drop surface.

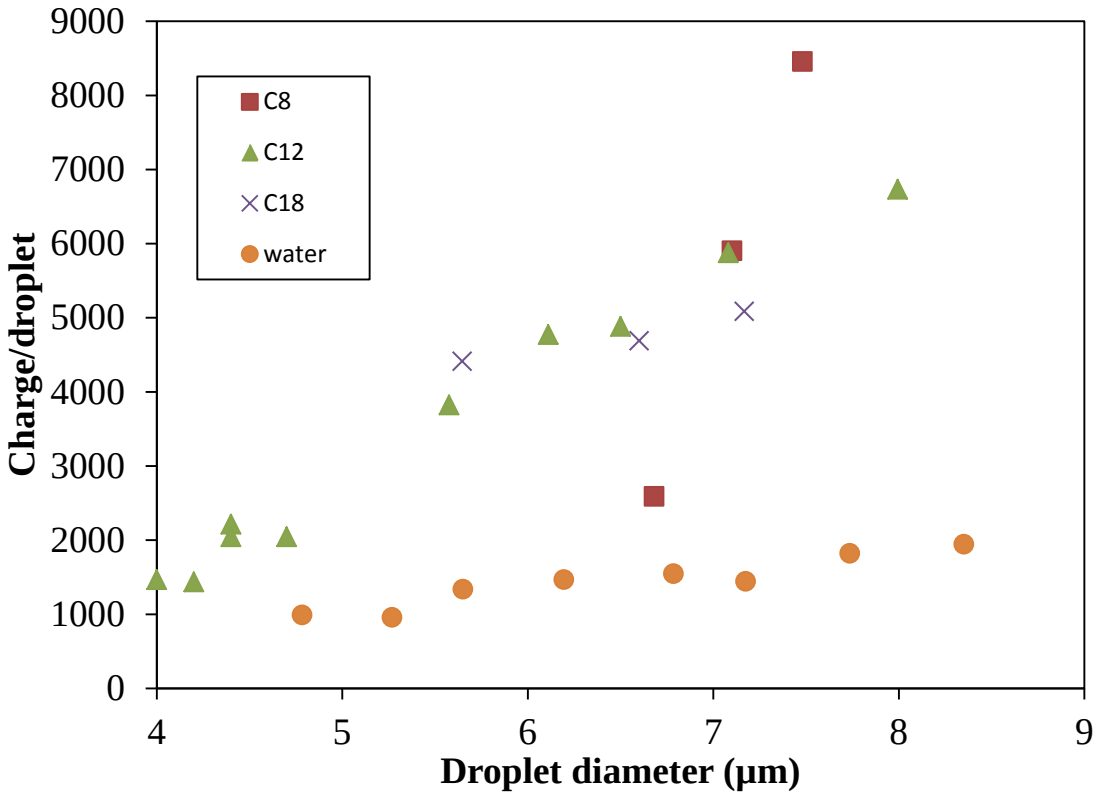


Figure 5-6: Data for all three anionic surfactants is presented. For all three surfactants, charge per droplet versus drop diameter is greater than water, with the shortest molecule showing the greatest enhancement.

### 5.2.5 Surface Charge for UAS Power Setting of 3.8 Watts

A lingering question surrounding our results was why an excess of positive charges on our droplets was seen when the theory of the electrical double layer (EDL) predicts that droplets should have an excess of negative charges. Data presented in Figure 5-7 is an attempt to answer this question. In Figure 5-7, we show that by altering the power level of the Ultrasonic Atomizing Sprayer, we are able to alter the polarity of the generated droplets.

Investigators such as Polat et al., Chein et al., and Zilch et al. report an excess of positive charges on generated droplets, but made no mention of why their results are not in line with the general consensus that generated water droplets should have a negative charge. To shed light on the question, the work of Matteson (1971) and Zilch (2008) was reviewed again. Matteson showed the rate of droplet formation can determine droplet polarity. As stated in Section 2.5, Matteson showed that increasing the velocity of the air jet breaking up liquid into droplets led to a reduction of negative charge on the droplets, which implied that the EDL is not being re-established as quickly as the droplets are formed at higher air velocities. Zilch's work showed that droplets formed from an air-jet sprayer had a higher positive droplet charge than those from a Vibrating Orifice Aerosol Generator (VOAG). An air jet sprayer will break up liquid into drops faster than a VOAG.

In an effort to answer this question, we decided to run a set of experiments with a reduced power level to our Ultrasonic Atomizing Sprayer (UAS). We found was that when the power level set point on the UAS is reduced to 3.8 W, the polarity of droplets becomes negative, and the magnitude of charge is reduced. Our results also show the charge per

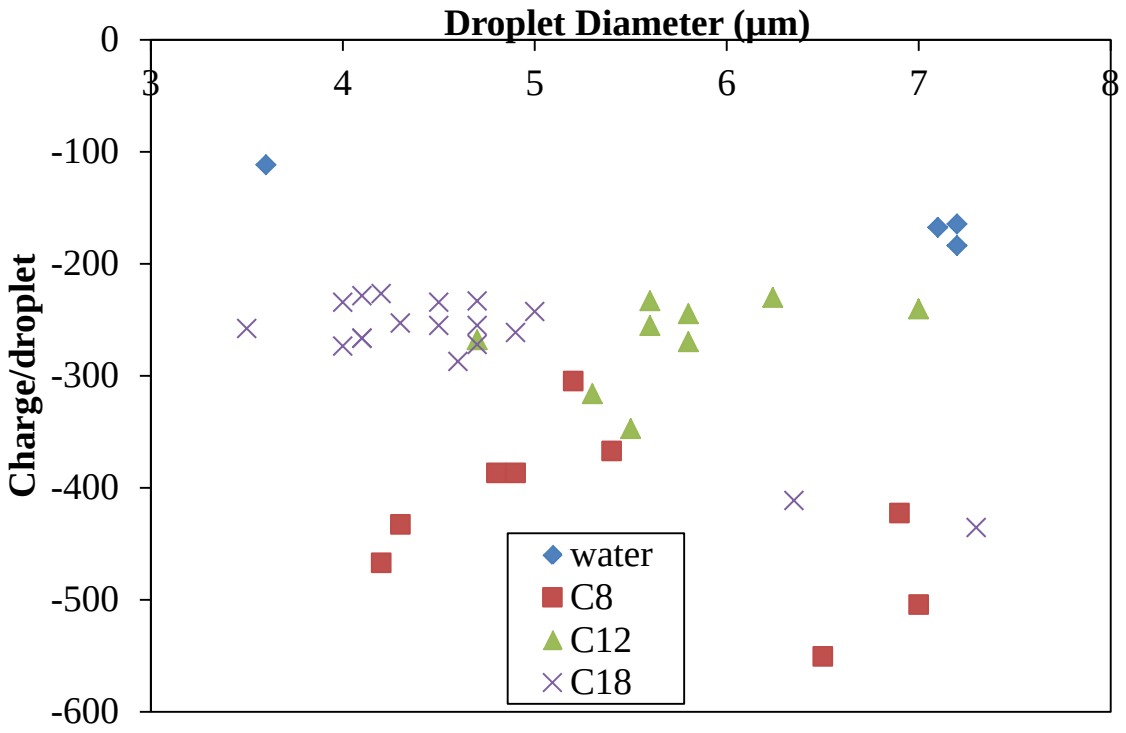


Figure 5-7: A sprayer power level of 3.8 Watts was used to generate droplets of all three anionic surfactants test as well as water. All droplets had an excess of electrons and the greatest charge enhancement was for the C8 compound.

droplet for the aqueous surfactant becomes negative at a sprayer power setting of 3.8 W. A charge enhancement is seen is for the surfactant solutions as well. See Figure 5-7. When comparing data generated by the UAS at the two different power settings of 3.8 and 6.8 W, one sees that all the data is negative. This shows that the rate of liquid break-up is the key factor in determining the polarity of the droplets generated. The data also shows a similar trend to what was seen with a power level of 6.8 W, that being that the anionic surfactants enhance charge compared to water and that the sodium octyl sulfate (SOS) again shows the greatest enhancement of charge.

## 5.3 Surface Charge on Droplets from the Vibrating Orifice Aerosol Generator (VOAG)

The VOAG was the second droplet generator used in this study, and the data are presented in Figure 5-8. We chose to experiment with the VOAG because we wanted to determine if liquid break-up/droplet generation with the VOAG would cause and excess of negative or positive charges on the droplet surface. Also, since it was clear that sodium octyl sulfate (SOS) shows the greatest charge enhancement in previous experiments, results presented in Figure 5-8 include data for SOS solutions tested with the VOAG as well.

The VOAG will generate a monodisperse droplet stream. The size distribution of droplets generated with the VOAG versus the Ultrasonic Atomizing Sprayer (UAS) is presented in Chapter 4. The reason for any size distribution with droplets from the VOAG is that evaporation rates differ from droplet to droplet. If this were not the case, droplets from the VOAG would be represented in a histogram by a single vertical line indicating only one droplet size. Even with differing evaporation rates, the droplet distribution presented in Chapter 4 for VOAG data is narrow compared to UAS data.

Droplet charge measurement experiments with the VOAG were performed with water and sodium octyl sulfate (SOS) solutions. Again, the SOS was selected based on results from the UAS showing that the shortest chain surfactant gave the greatest charge enhancement. Concentrations of $1 \times 10^{-6}$ M, $1 \times 10^{-5}$ M, and $1 \times 10^{-4}$ M of the C8 were tested. Figure 5-8 shows the results.

Water droplets showed less than 400 charges per droplet, with the exception of the single data point at 1524 charges per droplet. Droplet charge enhancement was observed for both the $10^{-5}$ M and the $10^{-6}$ M solutions of the C8. The $10^{-6}$ M solution had charge levels

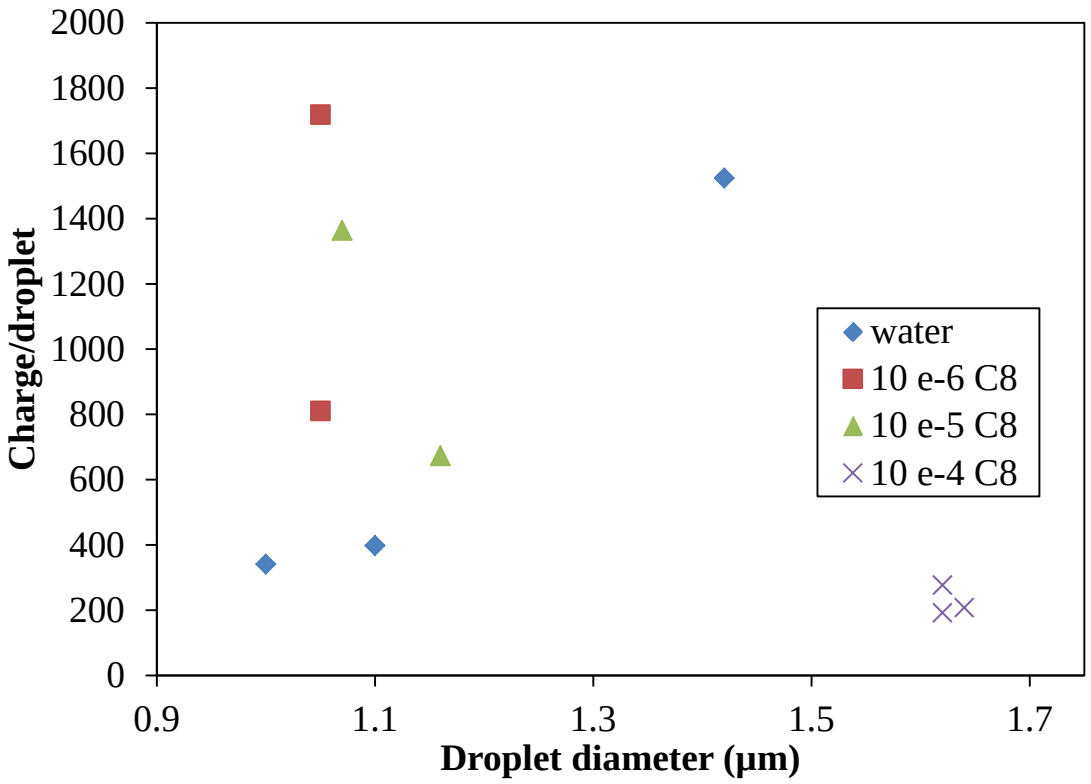


Figure 5-8: Drop data from three different sodium octyl sulfate concentrations, as well as water, are plotted. The $10^{-4}$ M solution of the surfactant showed no charge enhancement, but the $10^{-5}$ M and $10^{-6}$ M showed a distinct enhancement.

of 800 and 1719 charges per droplet, with the $10^{-5}$ M solution yielding values of 673 and 1364 charges per droplet. The $10^{-4}$ M solution of SOS showed the lowest charge per droplet. Recall that Polat reported a decrease in surface charge as surfactant concentration increased above 5 x $10^{-5}$ M, which he attributed to the surfactants starting to self-assemble and diffusion less to the droplet surface. Our results with the UAS also showed decreasing droplet charge with increasing surfactant concentration above 1 x $10^{-4}$ M. The trend of the majority of VOAG data is comparable to the data from the UAS, and is also similar to results reported by Polat (2000 and 2002) and Chein (2004).

## 5.4 Discussion

In the Introduction of this work, it was proposed that three factors control the magnitude of excess charges of a spray droplet. Those factors are number of ions per unit surface area for a given molecule, depth of the charge layer, which is related to the length of the molecule, and the flux of ions to the droplet surface. It was also proposed that the polarity of the excess charges could be modified based on the method of droplet generation. Regarding the number of surfactant ions per unit of surface area due to a given molecule, investigators such as Matteson, Polat et al., and Chein et al. reported the greatest increase in surface charge enhancement was observed with surfactants having straight-chain (normal) hydrocarbon groups in the molecule. These investigators stated this enhancement was due to less steric hindrances on the droplet surface for a straight-chained molecule, leading to an increase in molecules per unit area on the droplet surface. Our results with respect to this objective were inconclusive. In investigating this objective, we tested cocoamine versus sodium decyl sulfate. No definitive trend is seen that will allow us to say if steric hinderances play a role in increasing charge per droplet. In retrospect, the selection of these two molecules for a steric hindrance study was poor, but we could not directly purchase a branched SDS. Varadaraj studied surface tension differences of branched versus straight chain SDS, but he synthesized his own branched SDS, and we did not have the ability to do this.

The second factor that affects surface charge is the depth of the charge layer, which is dependent on the length of the surfactant molecule. Information in the literature is very limited to support this theory, with only Iribarne and Mason proposing that charge layer depth will enhance surface charge. The length of a surfactant molecule is on the order of

a few angstroms, which is small compared to droplet diameters of a few microns, but the results from several experiments we conducted support this theory. With the exception of our VOAG data, the shortest molecule used in our experiments, sodium octyl sulfate, consistently showed the greatest charge enhancement on droplet surfaces, with the longest molecule, sodium octadecyl sulfate showing the lowest charge enhancement. This trend held for both UAS power settings. The cocoamine results were not considered at this stage of the analysis due to the poor reproducibility of the CAM data.

Objective three involved the influence of molecular flux on surface charge enhancement. The reader is asked to recall the theories presented by both Myland and Matteson. It is a fact that smaller molecules will move through a given liquid faster than a larger molecule, if the molecules are similar in structure, as is the case with our three anionic surfactants. Both Myland and Matteson stated that molecular flux of ions will control the amount of excess charges on a droplet surface. Myland attempted to prove this by solving a form of the Poisson-Boltzmann equation for radial charge distribution, and Matteson attempted to prove this by showing results in which the smaller sodium dodecyl sulfate (SDS) molecules generated higher droplet charge versus the larger Catanac SP molecule. In Matteson's results, steric hinderances could have played a role in causing SDS to show higher charge than the Catanac molecule, but his work does not shed light on this question. With our results, we observed a greater surface charge enhancement with the smaller SOS molecules versus the SDS and SODS. In reality, determining whether the greater enhancement is due to the SOS diffusing faster to the surface, or due to its shorter length allowing more packing at the surface cannot be done at point. This question will be left for future investigators to answer.

While it was not an objective of our experiments initially, we quickly began to question why some investigators report negatively charged water droplets, and others report droplets with an overall excess of positive charges. The majority of our results show an excess of positive charges on droplet surfaces. We were not concerned about this since others report positively charged droplets, but we could not initially explain this. The only theory on natural droplet charging presented in the literature is that of the electrical double layer (EDL) that states drop charge should be negative. It was not until we performed experiments with lower power settings on our sprayer, coupled with a revisit of the work by Jonas and Mason, that we started to theorize that the polarity of generated drops is affected by not only the EDL theory, but equally as much as the relaxation time of the double layer.

In conclusion, droplet polarity can be manipulated by the rate of liquid break up. A faster break up rate tends to make droplets positive, while a slower break up rate causes drops to be negative. We can also conclude that shorter molecules will enhance droplet surface charge more than a longer molecule of similar structure. Whether this increased enhancement is due to faster diffusion or a higher packing at the surface cannot be determined at this time.

# Chapter 6
# Conclusions and Future Work

A charge measurement system was constructed and used to test surface charge on water droplets and aqueous surfactant droplets. We were able to show that surfactants enhanced surface charge, with the greatest enhancement observed with the sodium octyl sulfate due to its smaller structure allowing greater ion mass at the surface and the fastest diffusion rate to the droplet surface.

While our results prove our theories to a certain extent, more work is needed to determine which factor, or factors, plays the biggest role in surface charge enhancement. It is not seen from our results if surfactant packing at the surface is highest for straight chain molecules versus branched molecules. Other investigators were able to show this though. Which factor plays a bigger role in charge enhancement between the diffusion rates through the bulk water droplets, or the depth of the surface charge, is not known. Both factors are influenced greatly by the shorter molecule. A shorter molecule will lead to a thinner droplet surface layer and increased ion concentration close to the surface, which Iribarne and Mason's Equation 2.7 states is inversely proportional to droplet charge, but the shorter molecule will also diffuse to the droplet surface faster than a larger molecule with similar functional groups. Experiments need to be devised to investigate which of these two factors have a greater influence on droplet charge.

A second area in which further work needs to be done is in mathematical modeling of the variables that affect droplet charge. Varadaraj et al. (1992) and Evans (1999) relate surface tension to entropy of absorption to predict the effects of concentration on changes in surface tension, and it is felt that these variables could be used to predict the magnitude of surface charge enhancement in spray droplets.

Finally, more testing is needed with the cocoamine (CAM). The CAM showed charge enhancement, but there are challenges in working with CAM. If these difficulties could be overcome, CAM could be an effective surfactant since it is not a bulky molecule, although more bulky than the SDS tested. There are other CAM molecules with similar structures but not as long. A test matrix with three CAM molecules could be done to quantify the charge enhancement potential of CAM molecules.

Experiments should also be performed with a branch-chained sulfate surfactant similar to the anionic molecules tested in this study. The results would show if a normal chain surfactant will enhance surface charge more than a branched molecule.

# Bibliography


Baron, P. (1986) *J. Aerosol Sci.* **5**, 55.

Berglund, R., Liu, B. (1973) *Environmental Sci. and Technology*, **7**, 147.

Bird, R., Stewart, W., Lightfoot, E. (2007) *Transport Phenomena*, Wiley, New York.

Blanchard, D. (1958) *Journal of Atmospheric Sci*., **15**, 383.

Blanchard, D. (1963) *Progress in Oceanography* **1**, 73.

Bryne, M. J. (1977) *Studies on Spray Electrification and the Inertial Collection of Particles by Spheres*, Ph. D. thesis, University of Ireland.

Chein, H., Aggarwal, S., Wu, H. (2004) *Environ. Sci. Technology*, **38**, 5762.

Dahanayake, M., Cohen, A., Rosen, M. (1986) *J. Physical Chem*. **90**, 2413.

Dhariwal, V., Ray, A. K., Hall, P.G. (1993) *J. Aerosol Sci.* **24**, 197.

Elster, Geitel (1890) *Wied. Ann*., **39**, 321.

Evans, D., Wennerstrom, H. (1999) *The Colloidal Domain*, Wiley-VCH, New York.

Fuchs, N. (1964). *The Mechanics of Aerosols*, Pergamon, Oxford.

Hinds, W. (1982) *Aerosol Technology*, Wiley, New York.

Iribarne, J., Mason, B. (1967) *Trans. Faraday Soc*., **63**, 2234.

Jokanovic, V., Janackovic, D., Uskokovic, D. (1999) *Ultrasonics Sonochemistry*, **6**, 157.

Jonas, P.R., Mason, B.J. (1968) *Trans. Faraday Soc*, **64**, 1971.

Kim, J., Kim, D. (1997) *Environmental Engineering Res*. **2**, 279.

Koenigsberger, L., (1906) *Hermann von Helmholtz*, Clarendon, Oxford.

Kraemer, H.F., Johnstone, H.F. (1955) *Ind. Eng Chem*.**47**, 2526.

Kwetkus, B., Sattler, K., Kunzli, H. (1993) *Applied Surface Sci*., **68**, 139.

Lenard, P. (1892) *Ann. Phys.* **46**, 584.

Lippman, M. (1977) Regional deposition of particles in the human respiratory tract. Supplemental Ed. *Handbook of Physiology*, 2nd Edition.

Marangoni, C., (1871) *Ann. Phys. Chem*., **143**, 337.

Marra, W., Coury, J. (2000) *Brazilian J. of Chem. Eng*., **17**, 39.

Marra, W., Coury, J. (2009) *Powder Technology*, 191, 299.

Matteson, M. (1971) *J. Colloid and Interface Sci*., **37**, 879.

Mukherjee, A., Gidaspow, D., Wasan, D. (1987) *American Chemical Society, Division of Fuel Chemistry*, **32**, 395.

Myland, J. Oldham, K. (2002) *J. Electroanalytical Chemistry*, **522**, 115.

Mysels, K. (1986) *American Chemical Soc*., **2**, 423.

Nielsen, K., Hill, J. (1976) *Ind. Eng. Chem*., **3**, 149.

Nielsen, K., Hill, J. (1976) *Ind. Eng. Chem*., **3**, 157.

Periasamy, R., Clayton, A., Lawless, P., Donovan, R., Ensor, D. (1991) *Aerosol Science and Technology*, **15**, 256.

Peters, T., Leith, D. (2003) *J. Aerosol Sci*., **34**, 627.

Polat, M., Polat, H., Chander, S., Hogg, R. (2002) *Part. Part. Syst. Charact*., **19**, 38.

Polat, M., Polat, H., Chander, S. (2000) *J. Aerosol Sci*., **5**, 551.

Reischl, G., John, W., Devor, W. (1977) *J. Aerosol Sci*., **8**, 55.

Vaaraslahti, K., Laitinen, A. (1999) *J. Aerosol Sci*., **30 Sup. 1**, S693.

Vaaraslahti, K., Laitinen, A., Keskinen, J. (2000) *J. Aerosol Sci*., **31 Sup. 1**, S859.

Vaaraslahti, K., Laitinen, A., Keskinen, J. (2002) *J. of the Air and Waste Management*, **52**, 175.

Varadaraj, R., Bock, J., Zushma, S., Brons, N. (1992) *Langmuir*, **8**, 14.

Zeller, H. W. (1983) *Laboratory Tests for Selecting Wetting Agents for Dust Control*,

U.S. Bureau of Mines.

Zilch, L., Maze, J., Smith, J., Ewing, G., Jarrold, M. (2008) *J. Phys. Chem*., **112**, 13352.

Zuiderweg, F., Harmens, A., (1958) *Chemical Eng. Sci*., 9, 89.

# Nomenclature

| | |
|---|---|
| $a$ | acceleration of flow field ($m/s^2$) |
| $C$ | Cunningham correction factor (dimensionless) |
| $c$ | Concentration (M or mol/L) |
| $D_D$ | Droplet Diameter (m) |
| $dS$ | Differential surface area ($m^2$) |
| $e$ | elementary unit of charge ($1.6 \times 10^{-19}$ Coulombs/charge) |
| $\boldsymbol{F_e}$ | Electrical forces acting on the particle (N) |
| $f$ | Frequency of oscillation (Hz) |
| $f_B$ | Boltzmann voltage factor (32.9/V) |
| $I$ | Current (Ampere) |
| $J$ | Particle flux to surface of collector ($droplets/m^2 \cdot s$) |
| $K_E$ | Electrostatic Parameter for Coulombic Interaction (dimensionless) |
| $k_B$ | Boltzmann constant ($1.38 \times 10^{-23}$ J/K) |
| $N$ | Number density of droplets or particles in bulk gas ($droplets/m^3$) |
| $n_-$ | Anion number density ($\#/m^3$) |
| $n_+$ | Cation number density ($\#/m^3$) |
| $\eta$ | Collection efficiency (dimensionless) |
| $Q$ | Volumetric flow rate ($m^3/s$) |
| $Q_C$ | Charge per collector |
| $Q_D$ | Charge per droplet |
| $Q_P$ | Charge per particle |
| $q_e$ | Bulk gas flow rate ($m^3/s$) |
| $R_C$ | Radius of collector (m) |
| $R_D$ | Radius of droplet (m) |
| $R_P$ | Radius of particle (m) |
| $T$ | Temperature (K) |
| $U_0$ | Free stream gas velocity (m/s) |
| $U_r$ | Relative velocity between collector and particle (m/s) |
| $\boldsymbol{u}$ | Velocity of bulk fluid velocity (m/s) |
| $V_{TS}$ | Terminal settling velocity (m/s) |
| $\boldsymbol{v}$ | Velocity of particle (m/s) |
| $z_-$ | Negative charge number of ions from dissociated electrolyte |
| $z_+$ | Positive charge number of ions from dissociated electrolyte |
| $\varepsilon_A$ | Dielectric constant of the aqueous solution ($Coulombs^2/N \cdot m^2$) |

| | |
|---|---|
| $\varepsilon_0$ | Dielectric constant of the surrounding fluid (Coulombs$^2$/N·m$^2$) |
| $\mu$ | Viscosity of bulk fluid (kg/m·s) |
| $\rho_d$ | Density of droplet (kg/m$^3$) |
| $\rho_p$ | Density of particle (kg/m$^3$) |
| $\varphi$ | Local electrical potential in the droplet (V) |

# Vita

**Author's name** – Mark T. Warren

**Birthplace** – Dallas,Texas

**Birthdate** – July 15, 1970

**Education**

Master of Science in Chemical Engineering - Aerosol Science
University of Kentucky
May – 2012

Bachelor of Science in Chemical Engineering
University of Kentucky
December – 2000

**Professional Experience**

Cummins Engine Company
Columbus, IN
7/11 - present

University of Kentucky
Lexington, KY
1/10 - 7/11
Graduate Research Assistant

University of Kentucky
Lexington, KY

3/07 – 1/10
Research Engineer

The Okonite Wire and Cable Company
Richmond, KY
8/00 – 3/07
Process Engineer